or only in one hemisphere. If we observed FIRDA or FSWs at least once by EEG, we judged the recording as positive.

2.3. Data analyses

The age, gender, duration of illness and scores of WAIS-R between the two groups were analyzed statistically by the Mann–Whitney U test. The difference in the frequency of abnormal findings in EEGs was also statistically evaluated by Fisher's exact test ($p < 0.05$ was considered to be statistically significant).

The sensitivity, specificity, and positive and negative predictive values of FSWs for differentiating CBD from PSP, were determined as measures of the diagnostic accuracy. Sensitivity was defined as the percentage of cases with FSWs among all CBD cases diagnosed by the criteria discussed above. Specificity was defined as the percentage of cases without FSWs among all PSP cases diagnosed by the aforementioned criteria. Positive predictive value was the percentage of CBD cases among all cases with FSWs. Negative predictive value was the percentage of PSP cases among all cases without FSWs.

3. Results

3.1. Clinical findings

Clinical characteristics of CBD and PSP patients are summarized in Table 1. No significant differences were observed in age (CBD, median 63 (range: 50–74) years old; PSP, median 67 (range: 44–77) years old; $p = 0.472$), gender (CBD, M/F = 4/7; PSP, M/F = 4/10; $p = 0.977$) and duration of illness (CBD, median 24 (range: 7–36) months; PSP, median 24 (range: 6–48) months; $p = 0.977$) between the two groups. In clinical aspects, all CBD patients showed laterality of neurological signs including apraxia; however, no PSP patients revealed laterality or apraxia. Although alien limb syndrome is a distinct neurological sign in CBD, only 2 patients showed it and no PSP patient had this sign. No significant difference was observed in the WAIS-R between the two groups (CBD, VIQ 87.3 ± 11.2, PIQ 74.4 ± 16.5, TIQ 80.3 ± 12.9; PSP, VIQ 80.1 ± 12.1, PIQ, 69.6 ± 10.7, TIQ 73.7 ± 11.4; $p = 0.17$). On MRI, 9 of the 10 CBD patients had asymmetrical cortical atrophy, and 7 of the 14 PSP patients had brainstem atrophy. No patient showed any MRI abnormality, such as a cerebral infarction, that might influence EEG findings.

3.2. EEG findings

Representative EEGs in patients with CBD and PSP are shown in Figs. 1 and 2. In a representative CBD patient FSWs were observed in the right anterior temporal area (Fig. 1), whereas no FIRDA was seen. In contrast, a representative PSP patient revealed a typical FIRDA pattern without FSWs (Fig. 2).

Generally, there was no significant difference in the ratings of EEGs as performed by the two EEG specialists, especially regarding SBA, FSWs, and FIRDA. The results of EEG findings are summarized in Table 1. In general, most patients showed a preserved alpha rhythm at 8–11 Hz with the exception of one CBD patient and two cases of PSP, all three of whom showed SBA ($p > 0.99$). The frequency of FSWs was significantly different between the two

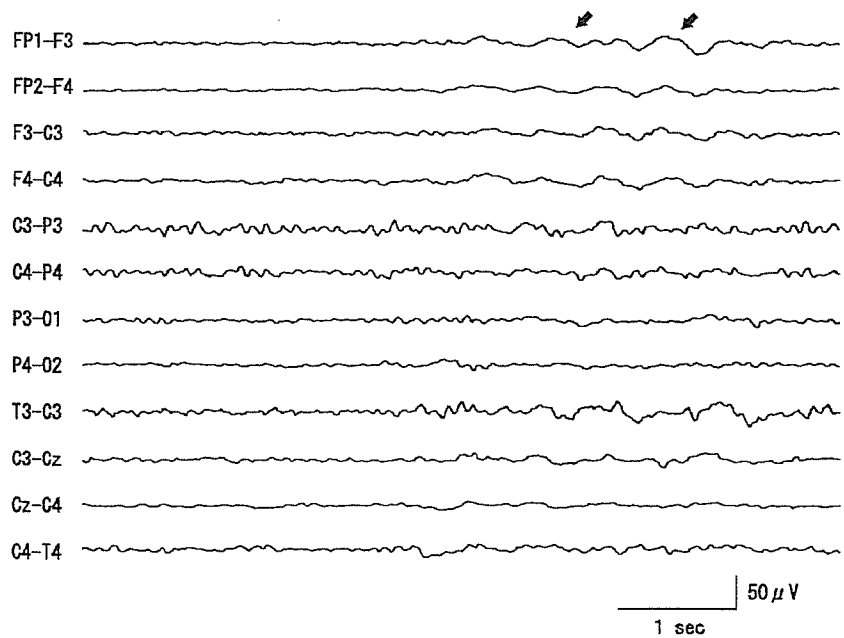

Fig. 2. Representative EEGs in a PSP patient (62-year-old, female; case 7). Note the bilateral synchronous frontal intermittent rhythmic delta activity (arrows). EEGs were recorded with a 14-channel analogue system.

diseases. FSWs were found in 8 patients (80.0%) with CBD, but only 2 patients (14.3%) with PSP ($p = 0.002$). FSWs appeared in the side contralateral to the dominantly-affected limb in 6 of the 8 CBD patients that showed this pattern. FSWs were found ipsilateral to the side of most atrophy on MRI in 7 of 8 CBD patients. In contrast, FIRDA occurred in 2 of the CBD patients (20.0%) and in 5 of the PSP patients (35.7%); however, there was no significant difference for FIRDA between the groups ($p = 0.357$). Two PSP patients and one CBD patient demonstrated both FIRDA and FSWs in the same EEG recording. Consequently, 9 of the PSP patients (64.3%) showed some kind of EEG abnormality, and 9 of the CBD patients (90%) showed EEG abnormalities ($p = 0.341$). No other abnormalities, such as sharp waves, spikes, photoparoxysmal responses and abnormal slow waves during hyperventilation, were seen in any patients Fig. 3.

Table 2
Sensitivity (*), specificity (**), positive and negative predictive values of FSW for differentiating CBD from PSP

	CBD	PSP	
FSW(+)	8	2	80.0%
FSW(−)	2	12	85.7%
	80.0%*	85.7%**	

We calculated the sensitivity of FSWs for differentiating CBD from PSP as 80.0%, the specificity as 85.7%, the positive predictive value as 80.0%, and the negative predictive value as 85.7% (Table 2).

4. Discussion

This is the first retrospective study to disclose characteristic EEG findings in the early-stages of CBD and PSP.

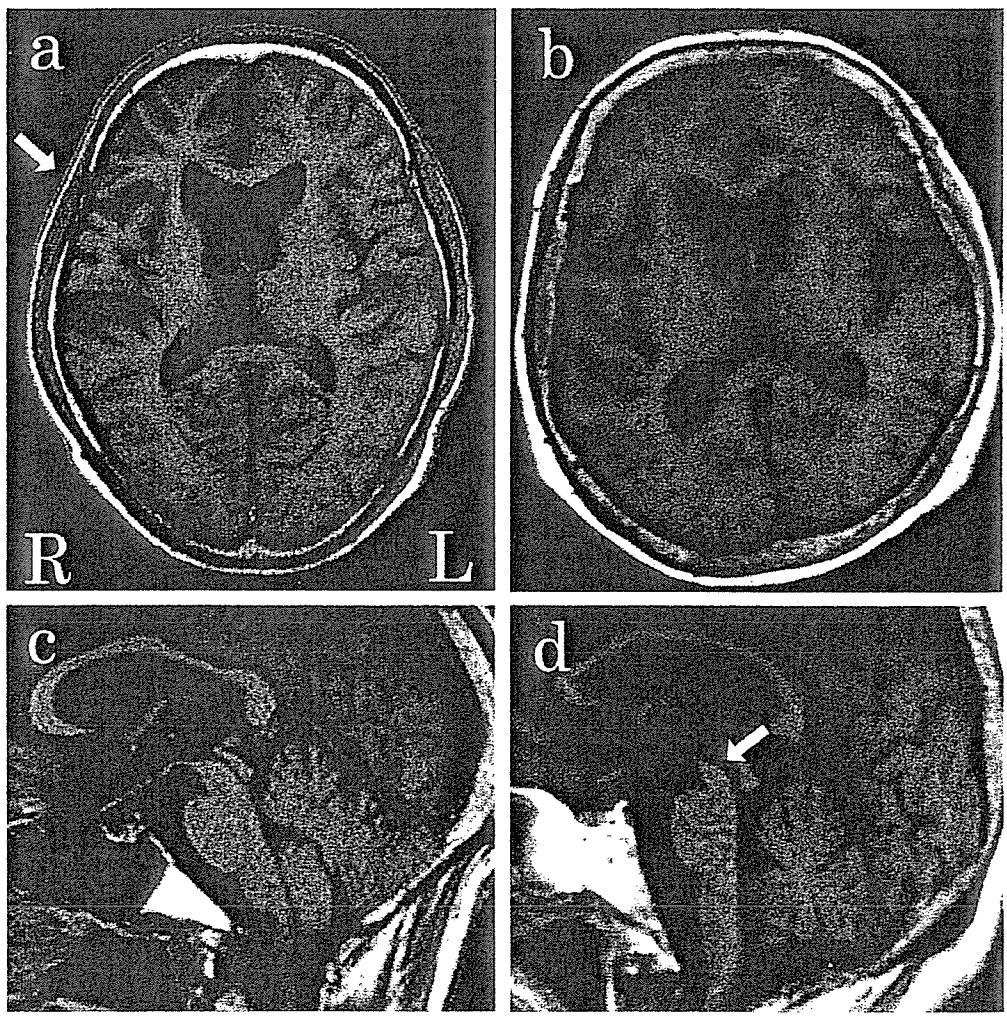

Fig. 3. Magnetic resonance imaging (MRI) images on a T1-weighted sequence (TR 500, TE 14) with axial views (a, b) and saggital views (c, d). The axial MRI shows marked cerebral cortical atrophy that is more pronounced in the right fronto-temporal lobe (arrow) in case 8 with CBD (a, arrow), whereas no asymmetry is seen in case 11 with PSP (b). The saggital view reveals marked atrophy of the midbrain (arrow) in case 11 with PSP (d), but not in case 8 with CBD (c).

Our results clearly showed that FSWs were significantly characteristic of CBD, but that FIRDA, which had been considered to be specific of PSP (Su and Goldensohn, 1973), was not a specific feature of that disease.

Our CBD patients showed asymmetrical neurological signs, FSWs in the affected side on EEGs, and asymmetric brain atrophy in parietal and frontal cortices by MRI. The laterality of FSWs was compatible with the clinical symptoms and MRI findings in CBD but not PSP. Previous neuropathological studies demonstrated that CBD has characteristic degenerative changes with asymmetry including neuronal loss, gliosis, and neuronal achromasia in the frontal and parietal cortices, and basophilic inclusions in cells of basal ganglia (Rebeiz et al., 1968; Gibb et al., 1989; Riley et al., 1990; Rinne et al., 1994). PET studies also showed an asymmetrical decrease in brain metabolism in cortical and subcortical regions in typical CBD (Eidelberg et al., 1991; Sawle et al., 1991; Nagasawa et al., 1996; Taniwaki et al., 1998). In general, polymorphic, irregular, and localized delta activity occurs mostly in the cortex overlying a circumscribed white matter lesion or, less commonly, in thalamic lesions (Gloor et al., 1977). Based on these findings, FSWs in our CBD patients are likely to concur with the atrophy and reduced metabolic rates, especially near the primary somatosensory cortex of the dominantly-affected side. On the other hand, only a few PSP patients showed FSWs, revealing a significant difference with CBD. Although there is no biological marker for either disease, and pathological findings are required to make a definitive diagnosis in both, there is as yet no consensus regarding the diagnosis of CBD (Litvan et al., 1996; Riley and Lang, 2000). Therefore, the presence of FSWs is potentially useful to distinguish CBD from PSP.

Unlike our results, most previous studies show a low frequency of FSWs in CBD (Table 3). This discrepancy may result from several factors. First, disease duration is relatively shorter in this study compared with that of others. Vion-Dury et al. (2004) reported a high frequency of FSWs (83%) in the Fourier transformed EEGs of relatively early-stage CBD patients. Thus, it is possible that FSWs are prominent at an early stage, but that they decrease in frequency with disease progression. Second, most studies did not focus on EEG, and EEG findings were not specifically mentioned. Third, specificity of CBD diagnosis will vary according to applied diagnostic criteria (Riley and Lang, 2000). Specificity of the diagnostic criteria used in this study is high enough so that false positive diagnosis is rare (Litvan et al., 1996; Riley and Lang, 2000).

On the other hand, FSWs occur in many normal elderly subjects. Silverman et al. (1955) found FSWs in about one-third of healthy volunteers > 60 years of age. These FSWs have been called the "benign temporal delta transients of the elderly", and have characteristics that occur mainly in the left temporal regions: sporadically as single waves or in pairs for only a very small proportion of the recording time, and the waves are usually rounded and < 60–70 μV (Klass and Brenner, 1995). FSWs in CBD patients were present ipsilateral to the side with most atrophy on MRI. In addition, they were not confined to the temporal region.

Several previous reports have performed electrophysiological comparisons between patients with CBD and PSP. CBD patients showed a significant prolongation of interpeak latency between N13 and N20 of short-latency somatosensory evoked potentials compared with PSP (Takeda et al., 1998). This finding indicates degeneration

Table 3
Comparison of EEG findings from the literature and the present study

Disease	Authors	Number of cases	Age (years)	Disease duration (months)	Asymmetric symptoms (%)	SBA (%)	FSWs (%)	FIRDA (%)	Asymmetric cortical atrophy on MRI/CT (%)
CBD	Rebeiz et al. (1968)	2	64–72	60, 72	100	0	0	0	NE
	Gibb et al. (1989)	1	69	24	100	0	0	0	100
	Riley et al. (1990)	8	61–77	48–120	100	50	13	0	50
	Lu et al. (1998)	2	64, 75	16, 20	100	0	0	0	100
	Manto et al. (2000)	1	56	24	100	0	0	0	100
	Vion-Dury et al. (2004)[a]	6	58–75	24–60	100	0	83	0	100
	Present study	10	50–74 (62)	7–36 (24)	100	10	80	20	90
PSP	Steele et al. (1964)	4	52–61	13–36	25	0	0	0	NE
	Su and Goldensohn (1973)								
	Initial	12	57–72	24–84	17	17	8	17	NE
	Follow-up	6	64–73	36–120	0	50	50	67	NE
	Fowler and Harrison (1986)	22	NS	NS	NS	0	NS	5	NS
	Torbjoern et al. (1989)	7	64–76	12–96	0	100	0	29	0
	Present study	14	44–77 (67)	6–48 (24)	0	14	14	36	0

[a] Fourier transformed EEGs were undertaken and the same diagnostic criteria as used in this study were adopted. Other reports did not specify their diagnostic criteria. SBA, slowing of background activity; FSWs, focal slow waves; FIRDA, frontal intermittent rhythmic delta activity; NE, not examined; NS, not specified; Numbers in parentheses represent medians.

of the supratentorial regions such as the thalamus or primary somatosensory cortex, because the distribution of brainstem lesions in CBD is similar to that in PSP (Paulus and Selim, 1990). Similarly, a study with cortical somatosensory evoked potentials (SEPs) reported myoclonus of cortical origin in CBD (Thompson et al., 1994). Therefore, the findings of focal supratentorial regions, such as the FSWs in EEG, could represent a hallmark of CBD.

Our current study revealed that the FIRDA pattern occurred in CBD as well as PSP. Su and Goldensohn (1973) reported that the EEG findings were almost normal in early-stage PSP, thereafter FIRDA appeared in 4 cases of 6 PSP patients (67%) during the follow-up period (Table 3). These 4 cases had typical clinical signs of PSP during the EEG recording period. Neuropathological findings in PSP show neuronal loss, gliosis, and neurofibrillary tangles in subcortical areas such as the globus pallidus, subthalamic nucleus, thalamus, substantia nigra, basis pontis, and dentate nucleus (Steele et al., 1964). Therefore, FIRDA in PSP has previously been considered to be a hallmark of subcortical lesions (Su and Goldensohn, 1973). However, a later EEG study (Fowler and Harrison, 1986; Table 3) found FIRDA in only one of 22 PSP cases. Not only diencephalic or infratentorial lesions, but also the diffuse cerebral structural lesions, focal structural lesions, or metabolic derangement, could result in FIRDA in the recent studies of a neuroimaging correlate of FIRDA (Fariello et al., 1982; Watemberg and Towne, 1997; Watemberg et al., 2002). These findings, as well as our results, suggest that the presence of FIRDA is not a useful parameter to use as a differential diagnostic tool for PSP and CBD.

In conclusion, CBD has an EEG feature distinct from PSP as determined by conventional EEGs. FSWs correlate with the neuro-anatomical and functional lesions most affected in CBD. Although the diagnostic value of applying EEG to an individual patient is limited, EEG could potentially be useful as a supplementary tool to distinguish CBD from PSP.

References

Eidelberg D, Dhawan V, Moeller JR, et al. The metabolic landscape of cortico-basal ganglionic degeneration: regional asymmetries studied with positron emission tomography. J Neurol Neurosurg Psychiatry 1991;54:856–62.

Fariello RG, Orreson W, Blanco G, et al. Neuroradiological correlates of frontally predominant intermittent rhythmic delta activity. Electroencephalogr Clin Neurophysiol 1982;54:194–202.

Fowler CJ, Harrison MJG. EEG changes in subcortical dementia: a study of 22 patients with Steele-Richardson-Olszewski (SRO) syndrome. Electroencephalogr Clin Neurophysiol 1986;64:301–3.

Gibb WRG, Luthert PJ, Marsden CD. Corticobasal degeneration. Brain 1989;112:1171–92.

Gloor P, Ball G, Schaul N. Brain lesions that produce delta waves in the EEG. Neurology 1977;27:326–33.

Kertesz A. Pick's Complex and FTDP-17. Mov Disord 2003;18(Suppl. 6):57–62.

Klass DW, Brenner RP. Electroencephalography of the elderly. Clin Neurophysiol 1995;12:116–31.

Litvan I, Agid Y, Calne D, et al. Clinical research criteria for the diagnosis of progressive supranuclear palsy (Steele-Richardson-Olszewski syndrome): report of the NINDS-SPSP international workshop. Neurology 1996;47:1–9.

Lu CS, Ikeda A, Terada K, et al. Electrophysiological studies of early stage corticobasal degeneration. Mov Disord 1998;13:140–6.

Manto M-U, Jacquy J, Van Bogaert P, et al. Rhythmic cortical and muscle discharges induced by fatigue in corticobasal degeneration. Clin Neurophysiol 2000;111:496–503.

Nagasawa H, Tanji H, Nomura H, et al. PET study of cerebral glucose metabolism and fluorodopa uptake in patients with corticobasal degeneration. J Neurol Sci 1996;139:210–7.

Paulus W, Selim M. Corticonigral degeneration with neuronal achtomasia and basal neurofibrillary tangles. Acta Neuropathol 1990;81:89–94.

Rebeiz JJ, Kolodny EH, Richardson EP. Corticodentatonigral degeneration with neuronal achromasia. Arch Neurol 1968;18:20 33.

Riley DE, Lang AE, Lewis A, et al. Cortical-basal ganglionic degeneration. Neurology 1990;40:1203–12.

Riley DE, Lang AE. Clinical diagnostic criteria. Adv Neurol 2000;82:29–34.

Rinne JP, Lee MS, Thompson PD, et al. Corticobasal degeneration: a clinical study of 36 cases. Brain 1994;117:1183–96.

Sawle GV, Brooks DJ, Marsden CD, et al. Corticobasal degeneration: a unique pattern of regional cortical oxygen hypometabolism and striatal fluorodopa uptake demonstrated by positron emission tomography. Brain 1991;114:541–56.

Silverman AJ, Busse EW, Barnes RH. Studies in the processes of aging: electroencephalographic findings in 400 elderly subjects. Electroencephalogr Clin Neurophysiol 1955;7:67–74.

Steele JC, Richardson JC, Olszewski J. Progressive supranuclear palsy: a heterogeneous degeneration involving the brainstem, basal ganglia and cerebellum with vertical gaze and pseudobulbar palsy, nuchal dystonia and dementia. Arch Neurol 1964;10:333–59.

Su PC, Goldensohn ES. Progressive supranuclear palsy: electroencephalographic studies. Arch Neurol 1973;29:183–6.

Takeda M, Tachibana H, Okuda B, et al. Electrophysiological comparison between corticobasal degeneration and progressive supranuclear palsy. Clin Neurol Neurosurg 1998;100:94–8.

Taniwaki T, Yamada T, Yoshida T, et al. Heterogenity of glucose metabolism in corticobasal degeneration. J Neurol Sci 1998;161:70–6.

Thompson PD, Day BL, Rothwell JC, et al. The myoclonus in corticobasal degeneration. Evidence for two forms of cortical reflex myoclonus. Brain 1994;117:1197–207.

Torbjoern GN, Roger CD, Mahendra M, et al. Seizures in progressive supranuclear palsy. Neurology 1989;39:138–40.

Vion-Dury J, Rochefort N, Michotey P, et al. Proton magnetic resonance neurospectroscopy and EEG cartography in corticobasal degeneration: correlations with neuropsychological signs. J Neurol Neurosurg Psychiatry 2004;75:1352–5.

Wang L, Kuroiwa Y, Kamitani T, et al. Visual event-related potentials in progressive supranucelar palsy, corticobasal degeneration, striatonigral degeneration, and Parkinson's disease. J Neurol 2000;247:356–63.

Watemberg N, Towne AR. Radiologic correlations of frontal intermittent rhythmic delta activity. Epilepsia 1997;38(Suppl. 8):119.

Watemberg N, Alehan F, Dabby R, et al. Clinical and radiologic correlates of frontal intermittent rhythmic delta activity. J Clin Neurophy 2002;19:535–9.

ELSEVIER

Clinical Neurophysiology 117 (2006) 1414–1433

www.elsevier.com/locate/clinph

Invited review

Studies of human visual pathophysiology with visual evoked potentials

Shozo Tobimatsu [a,*], Gastone G. Celesia [b]

[a] *Department of Clinical Neurophysiology, Neurological Institute, Graduate School of Medical Sciences, Kyushu University, 3-1-1 Maidashi, Higashi-Ku, Fukuoka 812-8582, Japan*

[b] *Department of Neurology, Loyola University Medical Center, Maywood, IL 60153, USA*

Accepted 11 January 2006

Available online 3 March 2006

Abstract

Visual evoked potentials (VEPs) offer reproducible and quantitative data on the function of the visual pathways and the visual cortex. Pattern reversal VEPs to full-field stimulation are best suited to evaluate anterior visual pathways while hemi-field stimulation is most effective in the assessment of post-chiasmal function. However, visual information is processed simultaneously via multiple parallel channels and each channel constitutes a set of sequential processes. We outline the major parallel pathways of the visual system from the retina to the primary visual cortex and higher visual areas via lateral geniculate nucleus that receive visual input. There is no best method of stimulus selection, rather visual stimuli and VEPs' recording should be tailored to answer specific clinical and/or research questions. Newly developed techniques that can assess the functions of extrastriate as well as striate cortices are discussed. Finally, an algorithm of sequential steps to evaluate the various levels of visual processing is proposed and its clinical use revisited.

Keywords: Visual evoked potentials; Parallel visual processing; Visual cortical areas; Clinical uses; Diagnosis

1. Introduction

It is well acknowledged that visual evoked potentials (VEPs) are useful for investigating the physiology and pathophysiology of the human visual system, including the visual pathways and the visual cortex. VEPs can be used effectively in association with psychophysics to study both normal and abnormal visual function. Since Halliday et al. (1972) first applied pattern reversal VEPs clinically for the diagnosis of patients with optic neuritis, VEPs have been especially helpful in the evaluation of patients with suspected multiples sclerosis (MS). VEPs may detect abnormalities in patients with visual complaints but no objective findings on examination and in patients without visual symptoms. Although the importance and clinical relevance of parallel processing have been recognized in the late seventies (Bodis-Wollner and Hendley, 1977; Bodis-Wollner et al., 1977; Spekreijse et al., 1973, 1985), recent progress of VEPs in clinical neurophysiology is based on two concepts: (1) visual information is processed simultaneously via multiple parallel pathways or channels and (2) a functional specialization in the visual system exists so that different attributes of the visual scene are processed in an anatomically separate part of the visual cortex (Celesia and DeMarco, 1994; Celesia et al., 1996; Felleman and Van Essen, 1991; Tobimatsu et al., 2000; Tootell et al., 1996; Zeki, 1993). In this review, we summarize concepts of the recent human visual system and emphasize the physical properties of the visual stimuli that are important for stimulus selection. We will also discuss the technical aspects of recording VEPs at various levels of visual processing. Finally, the clinical uses of VEPs are revisited.

2. Functional anatomy and physiology of the human visual system

The foundations of the major visual pathways in the mammalian visual system (cats and monkeys), from their beginnings in the retina through thalamic nuclei to striate cortex and beyond, will be described. Although some of

* Corresponding author. Tel.: +81 92 642 5541; fax: +81 92 642 5545.
E-mail address: tobi@neurophy.med.kyushu-u.ac.jp (S. Tobimatsu).

1388-2457/$30.00
doi:10.1016/j.clinph.2006.01.004

these data have not yet been demonstrated in humans, data are generally believed to represent, or have some homologue to the physiology of the human visual system.

2.1. Receptive field organization of the retinal ganglion cells

The retinal function can be summarized as the transduction of light into nerve impulses via rod and cone photoreceptors and the encoding of visual information by the neuronal structures of the retina (amacrine, horizontal, bipolar and ganglion cells). Rods function for night vision whereas cones operate for daytime and color vision. We will focus on the pathways formed by the cones. The three types of cones, maximally sensitive to long (L-cone), middle (M-cone) and short (S-cone) wavelengths, are important for all daylight vision in human.

The retina can be divided into a central foveal and parafoveal region, and a peripheral region. The fovea subtends 5° of visual angle while the combined foveal-parafoveal area subtends approximately, 8° (Celesia, 1985). The fovea contains the highest density of cones (190,000/mm^2) and ganglion cells with a rapid fall of concentration toward the periphery where rods predominate. The output cells of the retina are the ganglion cells, which transmit the retinal image to the lateral geniculate nucleus (LGN). About 90% of the cells in the parvocellular (P) layers of the LGN are strikingly sensitive to differences in wavelength, whereas cells in the magnocellular (M) layers are poorly responsive to wavelength changes (Derrington et al., 1984; Livingstone and Hubel, 1988).

Signals from photoreceptors to ganglion cells converge to either on- center or off-center cells. An on-center ganglion cell is excited when light stimulates the center of the receptive field and inhibited when light stimulates its surround. This is called 'center-surround' receptive field organization of the cat (Enroth-Cugell and Robson, 1966). The distinction between the 'center' and 'surround', and hence their interaction, is the sharpest in the foveal ganglion cells. Such transformation of the visual signal assists higher centers in detecting weak contrasts and rapid changes in light intensity of the cat (Enroth-Cugell and Robson, 1966; Kuffler, 1953; Rodieck and Stone, 1965). In addition, ganglion cells are specialized for the detection of local contrasts and rapid changes in the visual image and wavelength information (Shapley and Perry, 1986). A hypothesis about the architecture of image processing is shown in Fig. 1 (Palmer, 1999). Center-surround cells in retina and LGN provide input to local spatial frequency analyzer in primary visual cortex (V1). V1 is also important for form, color, orientation, local motion and depth (Livingstone and Hubel, 1988; Trotter et al., 1992; Zeki, 1993). The outputs of V1 could then be integrated by later processes or interacted with higher visual areas to compute edges, surface curvature, textures, stereopsis, and so on (Palmer, 1999; Ungerleider et al., 1998).

The population of parafoveally located ganglion cells has larger receptive field 'centers' than the foveal population. It is estimated that the 'center' size of human foveal ganglion cells is approximately between 10′–20′ of arc based on the psychophysical and VEP studies (Campbell and Maffei, 1970; Harter and White, 1970; Kulikowski and Tolhurst, 1973; Meredith and Celesia, 1982; Smith et al., 2001). Receptive fields of the retina (De Monasterio and Gouras, 1975; Hubel and Wiesel, 1960; Tessier-Lavigne, 2000) and LGN (Wiesel and Hubel, 1966) of monkeys are radially symmetrical (i.e., show little or no orientation selectivity). A vertical or horizontal slit-like stimulus or grating pattern will be equally effective in the retina and LGN (Hubel and

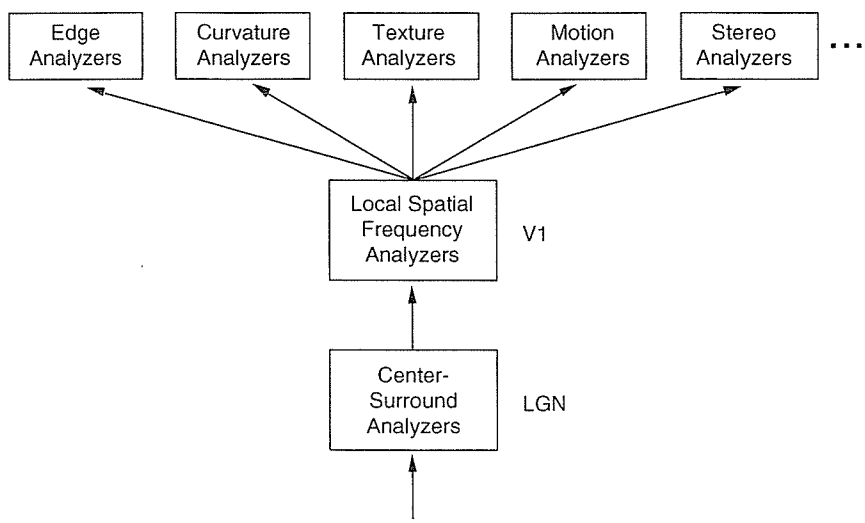

Fig. 1. A theoretical hypothesis about the architecture of image processing. Center/surround cells in retina and LGN provide input to local spatial frequency analyzer in area V1 of cortex, which then project their output to a variety of different modules that compute edges, surface curvature, textures, stereopsis, and so on, at later stages. (Adapted from Palmer, 1999).

Wiesel, 1968). In primates and humans orientation selectivity occurs in cortical neurons and not in LGN cells (Hubel and Wiesel, 1968; Maffei and Campbell, 1970).

2.2. Cortical visual areas

Approximately 25% of the human brain is involved in visual processing. Although it is not yet possible to subdivide the visual cortex with the same detail as has been achieved in monkeys, at least 10 cortical areas have been identified in humans by a combination of anatomical, functional and behavioral studies (Celesia, 2005; Tootell et al., 1996, 1997, 1998, 2003; Van Essen and Drury, 1997). Primate and human brains differ most in higher-order cortical regions and remain more similar in lowest-tier areas. In terms of cortical surface area, higher-order parietal, temporal, and frontal regions are expanded in human cortex, compared with the homologous cortical regions in monkey (Sereno and Tootell, 2005; Tootell et al., 2003).

Human V1 is similar to that of the monkey and corresponds to the cytoarchitectonic area 17 (Fig. 2). V2 roughly corresponds to cytoarchitectonic area 18 (Amunts et al., 2000; Kaas, 1989). Anatomic area 19 is a large cortical region that contains different functional areas, including area V3, V3a and VP (ventroposterior). Areas V3 and V3a (also named DM) are located dorsally or superiorly to the calcarine fissure above area V2. Tootell et al. (1997) have demonstrated that area V3a is "consistently crossing the transverse occipital sulcus" and is involved in motion processing. Within area 19, and including part of area 37,

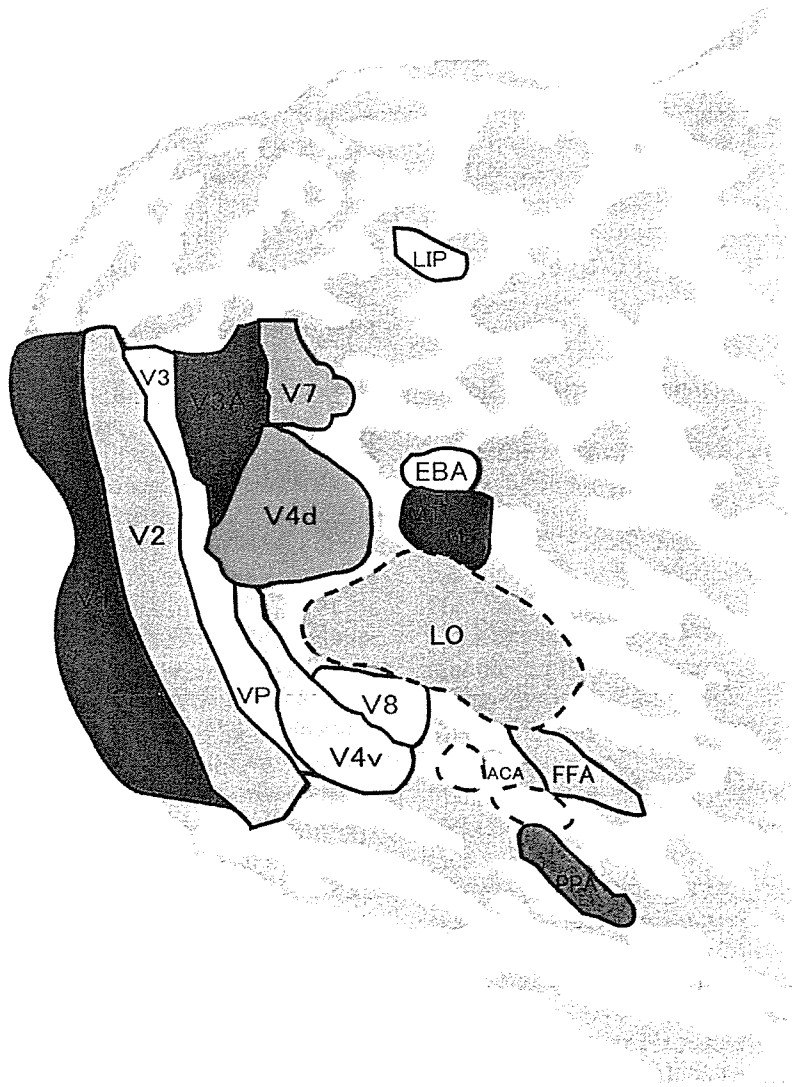

Fig. 2. Major cortical areas devoted to vision in human brain as studied by fMRI. This map shows the flattened cortical surface from right hemisphere reported by Tootell et al. (2003). See also Celesia, (2005), Downing et al., (2001), Malach et al., (1995) and Tootell et al., (1998) for more detail. Abbreviations: EBA: extrastriate body area, FFA: fusiform face area, LO: lateral occipital complex, MT: middle temporal area, MST: medial superior temporal area, LIP: lateral intraparietal area, PPA: parahippocampal place area, V3a: V3 accessory, V4d: V4 dorsal, V4v : V4 ventral, VP: ventral posterior area.

lies area V4. In human as well as primate there seems to be a visual area that analyses faces, this area is located in the fusiform gyrus and often close to the occipitotemporal sulcus. It has been proposed that the 'fusiform face area' is a module specialized for face perception (Allison et al., 1994, 1999; Downing et al., 2001; Kanwisher et al., 1997; Tootell et al., 2003) (Fig. 2). This region, however, also responds significantly to other categories of objects (e.g., houses, chairs and tools) (Haxby et al., 2001). Face perception may be mediated by a distributed cortical network that includes the inferior occipital gyrus, fusiform gyrus, superior temporal sulcus, hippocampus, amygdala, inferior temporal gyrus and orbitofrontal cortex (Ishai et al., 2005). There is also considerable overlap between the area that processes color and forms and the area that process faces (Allison et al., 1994, 1999). The lateral occipital complex (LO, Fig. 2) was also activated by objects and faces in the fMRI study (Malach et al., 1995). Thus, the boundaries of V4 in humans are unclear and the homologue of monkey V4 is not clear yet. There is also controversy whether the area processing color is lateral to the area processing faces as suggested by Tovee (1996) or mesial to it as suggested by Van Essen and Drury (1997). Cortical area V5 (also known as MT in monkey) is usually located in or near the posterior inferior temporal sulcus and often on the ascending limb of the inferior temporal sulcus (Van Essen and Drury, 1997).

2.3. Parallel visual pathways

Recent developments in neuroimaging such as positron emission tomography (PET), and functional magnetic resonance imaging (fMRI), in conjunction with new technologies in histology, have improved our understanding of human visual system (Celesia and Brigell, 1999a; DeYoe et al. 1994, 1996; Kaas, 1989; Tootell et al., 1996; Zeki et al., 1991). The human visual system consists of multiple, parallel channels which process different information, and each channel constitutes a set of the sequential process. Light increments (ON) and decrements (OFF), motion, stereoscopic depth, color, shape etc. are processed separately and simultaneously (Celesia and Brigell, 1999a; Celesia and DeMarco, 1994; Tovee, 1996; Zeki, 1993). The ON and OFF pathways segregate at the bipolar cells and proceed separately through the ganglion cells and the LGN to striate cortex (Schiller et al., 1986).

The optic nerve contains fibers from many types of ganglion cells including three major classes of cells. The midget cells represent about 80% of the ganglion cells and constitute the P-pathway while the parasol cells represent about 10% of the ganglion cells and comprise the M pathway (Celesia, 2005; Perry et al., 1984). The third pathway is called the koniocellular (K) pathway that originates form the small bistratified ganglion cells representing about 10% of retinal ganglion cells (Celesia, 2005). The 3 systems M, P, K remain segregated and terminate in separate layers in V1 via LGN and their functional properties differ from each other (Casagrande and Xu, 2004; Chatterjee and Callaway, 2003). The M-pathway is fast conducting and show a broad spectral sensitivity, and specialized for processing transient information. Thus, M-pathway has photopic luminosity function and is sensitive to stimuli with low spatial and high temporal frequencies (Dacey, 1999; Livingstone and Hubel, 1988). The P pathway is 'more sluggish and can process fine details', therefore, it is more sensitive to higher spatial and lower temporal frequencies, and process red–green (R–G) information in which L- and M-cone signals are antagonistic (Dacey, 1999; Dacey and Packer, 2003). The function of the K pathway is less clearly understood (Casagrande and Xu, 2004), but some of these cells contribute to blue-yellow (B-Y) information in which S-cones are opposed by a combined L+M-cone signal (Chatterjee and Callaway, 2003; Dacey, 1999; Dacey and Packer, 2003) and motion processing (Morand et al., 2000).

From V1 and V2 the three pathways (P, M, K) become intermingled by feedforward, feedback and lateral interactions. The two cortical visual pathways have been proposed: the ventral or temporal and the dorsal or parietal streams (Mishkin et al., 1983; Tootell et al., 1996). The ventral stream has also been called the 'what system' because it is involved in the identification of an object, whereas the dorsal stream is called the 'where system' because of its involvement in the processing of spatial location. It appears that the M and P pathways correspond approximately to the two systems with the P pathway projecting primarily to the ventral stream and the M pathway providing the primary input to the dorsal stream (Livingstone and Hubel, 1988). The M and P pathways coexist in V1 and V2 and signals from both pathways can be intermixed in the superficial layers of V1 (Ferrera et al., 1994; Lund et al., 1994). These two general processing pathways also exist in the human visual cortex (Tootell et al., 1996). V1 is often pictured as a giant railroad switching station. In this model, trains that come from LGN may be switched to different tracks but remain recognizable as they leave V1 station (Casagrande and Royal, 2003). The M (where) system projects to area V3 via V1 and V2, then to the medial temporal region V5, and terminates in the posterior parietal area 7a (Livingstone and Hubel, 1988). This system processes where stimuli are located and determines if they are moving. The P (what) system goes to area V4 via the parvo-blob and parvo-interblob pathways of V1 and then proceeds to the inferior temporal area 37 (Livingstone and Hubel, 1988). These areas are involved in the processing of visual form and color. However, there is considerable cross talk between the two systems: V4, unlike V5, receives strong input from both M and P pathways (Ferrera et al., 1992, 1994). Thus, the M and P pathways are not related in a one-to-one fashion to the dorsal and ventral streams of processing. The asymmetric sorting of M and P contributions to the dorsal and ventral streams represents an efficient method of transmitting low-level information, and

that the cortical streams draw on information coded in the M and P pathways according to their particular needs (Ferrera et al., 1994).

The functional specialization of separate anatomical areas is confirmed by the effect of selected lesions producing deficits limited to color, spatial perception or movement (Baker et al., 1991; Barton and Sharpe, 1997; Kraut et al., 1997; Zihl et al., 1991). However, we must be cautious that anatomical segregation is far from absolute, and some lesions limited to specific areas only produce a temporary effect with subsequent recovery. No single hypothesis so far can truly account for the complexity of visual processing. How can we reconcile the hypotheses of multiple parallel channels, functional specialization and hierarchical organization with the unitary, integrated phenomenology of visual experience? The hypothesis of a distributed network (Celesia et al., 1997; Mesulam, 1981) may bring these separate concepts together. The visual system is modular (Bartels and Zeki, 1998; Kaas, 1989): Modules are added as needed to increase information processing and each module operates via a distributed network with crucial nodal points (or information bottlenecks). The most crucial nodal point is V1 where all incoming information is received and then distributed to the other areas of the network. Lesions at crucial nodal points will produce specific visual deficits (e.g. homonymous hemianopia in V1 lesions). Lesions in the network may be silent or transient. Other modules or network connections may compensate for the damaged area (plasticity). An example of the latter is a lesion at V5 producing a partial impairment of visual motion perception (akinetopsia) (Regan et al., 1992).

3. Visual stimulation

3.1. Visual stimuli and their physical characteristics

The definition of the stimulus parameter is important to improve communication and to permit comparison of data among laboratories (Bodis-Wollner et al., 1986; Celesia and DeMarco, 1994). Pattern stimuli should be defined by: the type of pattern (gratings, bars and checks), their size or spatial frequency, their contrast, the size of the field of presentation, the mean luminance of the field and the luminance of the background, the type of pattern presentation (reversal or onset–offset), the temporal frequency of the reversal or presentation. The 'spatial frequency' (f) of a pattern is the number of bars or gratings subtended in an angle of one degree at the eye and is expressed in cycles per degree (cpd). The width (w) of a bar can be calculated by the formula $w=60/2f$, where w is in minutes of arc and f is spatial frequency in cpd. Conversely, the fundamental spatial frequency of a check pattern can be expressed as $f=60/1.4w$, where f is measured in cpd and w is the width of the check in minutes of arc. The mean luminance of the pattern is the average luminance in cd/m^2 of the screen and is expressed by the formula: $(L_{max} + L_{min})/2$ where L_{max} and L_{min} represent the maximum and minimum luminance value across the stimulus field. Contrast (C) is the luminance difference of adjacent dark and bright portion of the pattern and is expressed by the formula: $C = [(L_{max} - L_{min})/(L_{max} + L_{min})] \times 100\%$. Recent guidelines for proper calibration of stimulus and recording parameters have recently been published (Brigell et al., 2003).

As previously mentioned in 2.1., gratings and checks are preferred to explore the function of V1 because local spatial frequency analyzers are presumably present in V1 (Blakemore and Campbell, 1969; De Valois et al., 1979). By selecting the appropriate pattern element size, one can predominantly stimulate the fovea or the peripheral retina. Small size patterns somewhere between 10′ and 15′ of arc preferentially stimulate the fovea, while patterns subtending more than 30–40′ of arc stimulate both the fovea and extrafoveal region (Bodis-Wollner et al., 1986; Celesia, 1984). Pattern element position and its size are another important factors for determining the peripheral versus foveal stimulation due to the large cortical representation of the macula (cortical magnification). Scaled stimuli with eccentricity are expected to produce a signal of a similar order of amplitude from each stimulating segment (Baseler et al., 1994; Klistorner et al., 1998; Meredith and Celesia, 1982).

3.2. Transient versus steady-state stimulation

To generate VEPs, stimuli must be temporally modulated. The most commonly used method of stimulation is pattern reversal using either a checkerboard or a grating pattern (Regan, 1989). The other modes of presentation, flash VEPs and pattern onset VEPs, are less often used in clinical practice. Transient VEPs (T-VEPs) are obtained to a low stimulus rate. An evoked potential is elicited to each stimulus and the averaged responses being time-locked to the stimulus (Bodis-Wollner et al., 1986; Regan, 1989) and can be measured with their latency and amplitude (Fig. 3A). On the other hand, steady-state VEPs (S-VEPs) are elicited by repetitive frequent stimuli. The stimulated structures can no longer respond to each stimulus and the evoked waveforms become quasi-sinusoidal due to the overlapping responses with the number of deflections corresponding to the stimulus frequency (Fig. 3B) (Bodis-Wollner et al., 1986; Celesia, 1984; Regan, 1989). Fast Fourier analysis is often employed to study the phase and amplitude of the harmonic components of the S-VEPs (Fig. 3C, D). In general, the second harmonic response is the major component of pattern reversal S- VEPs due to nonlinearities in the visual system (Marx et al., 1986; Strasburger et al., 1993). The phase data showed small inter- and intra-subject variability (Tobimatsu et al., 1996). On the other hand, the amplitude data showed a large degree of inter-subject

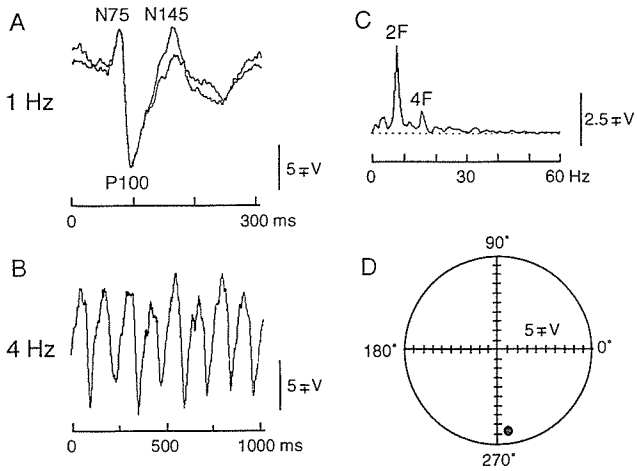

Fig. 3. Normal waveforms of transient and steady-state VEPs. Transient VEPs consist of three major components (N75-P100-N145) (A) whereas steady-state VEPs show quasi-sinusoidal waveforms, corresponding to the reversal frequency (8 reversals/s) (B). Fourier analysis yields the power spectrum and shows that the second harmonic response (2F, 8 Hz) is predominant (C) while the fourth harmonic response (4F) is relatively small. The amplitude and phase of the 2F component (●) are plotted in polar plots (D). (Adapted from Tobimatsu, 2003)

variability, although the intra-subject variability was very small. Phase is considered the analogue to the latency of T-VEPs (Strasburger et al., 1988; Tobimatsu et al., 1991).

For a linear system, the transient response has a fixed relationship to the steady-state response, however, visual pathways commonly show several types of nonlinear behavior (Bobak et al., 1988a; Bodis-Wollner et al., 1986; Regan, 1982, 1989; Shapley and Perry, 1986; Srebro, 1992; Zemon et al., 1986). Thus, transient and steady-state stimulation could produce responses that provide complementary information about the visual system. In clinical studies of multiple sclerosis (Celesia et al., 1992) and Parkinson's disease (Marx et al., 1986), S-VEPs were sometimes abnormal in patients with normal T-VEPs. S-VEPs are superior to T-VEPs when we investigate the temporal frequency function of the visual system. Therefore, a combined use of T-VEPs and S-VEPs may provide additional insights into the understanding of the human visual system (Regan, 1982; Tobimatsu, 2002b; Tobimatsu and Kato, 1998).

3.3. Variables affecting VEPs

The pattern stimuli are either back-projected by way of a rotating mirror to a translucent screen or displayed electronically on a cathode ray tube (CRT) monitor. Abrupt movement of the mirror produces almost instantaneous reversal of the pattern. In contrast, CRT monitors take 16.7 ms (at 60 Hz) to make one raster sweep and thus to complete the pattern reversal. As a result, VEP latencies for a CRT display are generally longer than those recorded with use of a mirror projection system (Aminoff and Goodin, 1994). Use of a liquid crystal display (LCD) may not be appropriate because distortions in luminance and contrast characteristics are more drastic than those of CRT monitors (Strasburger et al., 2001).

The latency and amplitude of P100 of T-VEPs are significantly affected by pattern luminance, contrast, spatial frequency content (or check size) and stimulus field size (Celesia, 1984; Chiappa, 1997). In brief, P100 latency increases as pattern luminance is decreased probably due to the reduction of the retinal illuminance (Tobimatsu et al., 1988). Decreased contrast causes amplitude reduction and latency prolongation (Chiappa, 1997; Tobimatsu et al., 1993a). P100 latency shows a U-shaped function against check size (Kurita-Tashima et al., 1991; Tobimatsu et al., 1993a). Approximately 80% of the pattern VEPs response arises from the central 8 degree of the stimulus field (Chiappa, 1997). Orientation of gratings is another important clinical variable (Arakawa et al., 2000; Camisa et al., 1981; Kupersmith et al., 1984). Age, sex and pupil size are other important variables affecting both amplitude and latency of VEPs (Bodis-Wollner et al., 1986; Celesia, 1984; Tobimatsu, 1995; Tobimatsu et al., 1988). There is a curvilinear relationship between the P100 latency and age (Celesia et al., 1987; Tobimatsu et al., 1993a). Females have shorter P100 latency and larger P100 amplitude than males (Celesia et al., 1987; Tobimatsu et al., 1993a). Pitt and Daldry (1988) suggested the following formulas applied for the two genders: Males P100 latency = 129.5–1.337(age) + 0.01808(age^2); Females P100 latency = 137.2–1.927(age) + 0.02489(age^2). The latencies of P100 show an increase of 2–3 ms/mm of decreased pupillary diameter while the P100 amplitude reveal a trend toward smaller amplitude as the pupil size becomes smaller. This is probably due to the reduced retinal illuminance. P100 showed an increase of 10–15 ms/log unit of decreased retinal illuminance (Tobimatsu et al., 1988).

4. Neural generators of VEPs

4.1. Source localization techniques

Magnetoencephalography (MEG) has an excellent temporal resolution in the study of the human brain activity. MEG has been used to localize the sources of measured brain signals but its localization is hampered by the nonuniqueness of the inverse problem (Hämäläinen et al., 1993; Stenbacka et al., 2002; Tobimatsu, 2005). Local currents can be accurately modeled with equivalent current dipoles (ECDs) that are described by their fixed 3-dimensional location, fixed orientation, and variable amplitude. Although single current dipoles adequately represent local active areas, multiple and overlapping sources form a challenge for MEG modeling. Thus, multi-dipole models with time-varying source strengths have been developed in several laboratories to better account for complex sources

(Aine et al., 2000; Hämäläinen et al., 1993; Stenbacka et al., 2002). Another type of commonly used source model divides the entire brain or just the cortex into a large number of grid sites (e.g., distributed source model). Minimum current estimate is an example of this model and explain the measured signals with a current distribution that has the smallest sum of current amplitudes (Ungerleider et al., 1998; Uutela et al., 1999). The same is true for EEG source localization, however, the inverse problem can be solved by introducing reasonable a priori constraints (see for review, Michel et al., 2004). On the other hand, fMRI has an excellent spatial resolution but relatively low temporal resolution compared with MEG/EEG. fMRI is currently the most widely used method for brain mapping and studying the neural basis of human cognition. The blood-oxygen-level-dependent (BOLD) signal of fMRI correlated well with the local field potentials but not spike activity, which suggests that the BOLD signal reflects the input and intracortical processing of a given area rather than the output signal transmitted to other brain regions (Logothetis, 2002). Therefore, a combined use of electrophysiology and fMRI provides more precise information about the anatomical origins of cortical activities (Di Russo et al., 2001, 2005). However, the existence of at least 10 cortical areas (VI, V2, V3, V3a, VP, MT, MST, V4v, V4d and V8, Fig. 2) with a retinotopic representation in humans must be taken into account in any explanation of the source of VEPs recorded from the scalp.

4.2. Pattern reversal transient VEPs

PR-VEPs are characterized by an initial small negative (N75), followed by a major positive wave (P100) and then by a negative wave (N145). The origin of P100 in the brain has been intensively studied by vision researchers, and has been suggested to originate in the occipital cortex (Barrett et al., 1976). Recently, MEG has been used to localize the sources of measured brain signals and there have been a number of studies regarding neural generators of pattern reversal visual evoked magnetic fields (PR-VEFs). PR-VEFs consist of N75m, P100m and N145m, corresponding in time to N75, P100 and N145 of PR-VEPs (Fig. 4a). Most studies have revealed that ECDs of the P100m are estimated in striate cortex (Hashimoto et al., 1999; Nakamura et al., 1997, 2000; Seki et al., 1996; Shigeto et al., 1998) (Fig. 4b). Interestingly, all studies have estimated the neural generator of the P100m by using the single-dipole model. Most studies also revealed the retinotopic organization of the P100m (Fig. 4c), which was consistent with the retinotopic organization of V1 (Nakamura et al., 1997; Seki et al., 1996; Shigeto et al., 1998).

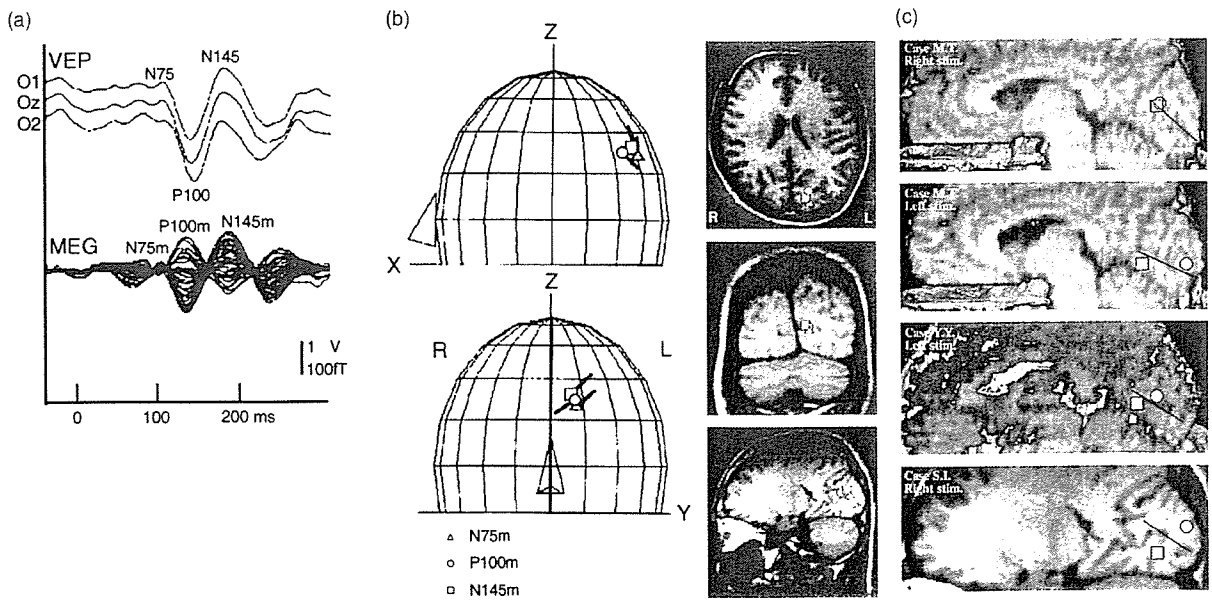

Fig. 4. An example of the simultaneous recording of PR-VEPs and VEFs to left half-field stimulation (a). PR-VEPs show well-defined N75, P100 and N145 (upper trace). VEF responses of 37 channels are superimposed (lower trace). Three major components, N75m, P100m and N145m are identified. The dipole localization of VEF for N75m, P100m and N145m is superimposed on a spherical model of the head and on MRI (b). The locations of the estimated dipoles of N75m (triangle), P100m (circle) and N145m (square) are shown (left). The localization of the three dipoles are close together in the occipital region contralateral to the stimulated right half-field. The lines attached to the estimated dipoles indicate the direction of the current flow. The current flow of the estimated dipole is from the medial to the lateral side for N75m and N145m, while that of P100m is toward the medial side. The dipoles of N75m, P100m and N145m are estimated within the cortex around the calcarine fissure on the contralateral side. The dipoles of N75m and N145m are located ventral and dorsal, respectively, in reference to the dipole of P100m. L: left, R: right. The dipole localization of P100m to the upper and lower quadrant field stimulation in subjects overlaid on MRIs (c). The open squares represent the location of the estimated ECD to the upper quadrant field stimulation while the open circles refer to the lower quadrant stimulation. Lines represent the calcarine fissure. The upper quadrant stimulation results in a dipole located in a more ventral part of the calcarine fissure, compared with lower quadrant stimulation (adapted from Shigeto et al., 1998).

ECDs of the N75m were estimated in striate cortex (Hashimoto et al., 1999; Nakamura et al., 1997; Shigeto et al., 1998) (Fig. 4b), however, ECDs of N145m were estimated in striate cortex (Hashimoto et al., 1999; Shigeto et al., 1998) or extrastriate cortex (Nakamura et al., 1997). The direction of the current flow of ECDs of N75m and Nl45m was from the medial to the lateral aspect of the head, whereas that for P100m was directed medially when viewed in a coronal section (Shigeto et al., 1998) (Fig. 4b). It is well known that the physiological properties of major components of PR-VEPs differ from each other. For instance, aging (Allison et al., 1984), check size (Kurita-Tashima et al., 1991) and binocular stimulation (Tobimatsu and Kato, 1996) differentially affected the latency and amplitude of each component. In addition, evoked responses to the pattern reversal stimulation recorded in the vicinity of optic tract in man (Tobimatsu et al., 1997) showed an initial positive deflection (P50) followed by a negative wave (N80). These findings suggest that N75 may represent an initial response of striate cortex and that major components of PR-VEPs are generated from the different neuronal populations in striate cortex.

4.3. Pattern onset transient VEPs

The transient pattern onset VEP elicited by a checkerboard pattern, square-wave gratings or sinusoidal gratings has three major components: CI (a negative peak at 65–80 ms), CII (a positive peak at 90—110 ms, or called P1) and CIII (a negative peak at 130–150 ms). There is a reversal of the polarity of each component in the VEPs obtained to upper and to lower half-field stimulation. For the lower half-field responses, the polarities of CI, CII, and CIII are generally positive, negative, and positive, respectively (Jeffreys, 1977). On the basis of topographical amplitude pattern and source analysis, CI is considered to originate in extrastriate cortex while CII is generated in striate cortex (Maier et al., 1987; Ossenblok and Spekreijse, 1991). However, the other investigators proposed that CI was originated in striate cortex (Butler et al., 1987; Di Russo et al., 2001; Jeffreys, 1977; Jeffreys and Axford, 1972a) while CII was an extrastriate origin (Di Russo et al., 2001; Jeffreys, 1977; Jeffreys and Axford, 1972a,b). CIII is assumed to be generated in extrastriate cortex (Di Russo et al., 2001; Jeffreys, 1977; Ossenblok and Spekreijse, 1991).

Unlike the results of PR-VEFs, source localization studies using MEG have also failed to demonstrate a single neural generator of CI and CII, respectively. Aine and colleagues (1990, 1995) reported that activation occurring around 80–90 ms was in or near striate and was followed by activation of extrastriate sources around 110–120 ms by using the two-dipole model. These findings suggest the asynchronous activation of multiple spatially separable sources around 100 ms. Tzelepi et al. (2001) estimated the source(s) of the early component with a peak latency of 70 ms. Although neither the single-dipole model nor the two-dipole model produced a good fit across runs, the application of magnetic field tomography identified overlapping activity in striate and extrastriate areas. Vanni et al. (2004) have used pattern onset VEPs with fMRI and multiple dipole analysis and found that V5 is activated 10–20 ms after V1 activation. Tzelepi et al. (2001) also found labile V5 and V6 activations after 30 ms V1 activation using MEG. These results are interesting, but it should be pointed out that the visual stimuli used in these studies do not selectively stimulate the dorsal pathway.

Part of the conflict in the literature is a consequence of attempts to relate components in the waveform across studies from different laboratories that have used very different stimuli. Stimulus types (checkerboard *vs* gratings), spatial frequencies (low *vs* high), contrast (low *vs* high), the location of the stimulus field (upper *vs* lower or right *vs* left), eccentricities (central *vs* peripheral) are important factors that have an impact on whether one sees CI and CII as predominantly a striate or extrastriate source (Aine et al., 1995; Jeffreys, 1977; Kenemans et al., 2000; Plant et al., 1983).

5. Functions of extrastriate visual cortices

The multiplicity of the extrastriate cortices in humans is slowly being unravelled and will require additional studies. In this section, we will limit our review to cortical areas processing color, face and motion.

5.1. Cortical areas responsive to color and face stimuli

As previously mentioned, the P pathway carries information of R–G color while the K pathway conveys B–Y information. Form perception is performed by both P and M pathways: the former is responsible for high spatial frequency information in visual images while latter is important for low spatial frequency information (Vuilleumier et al., 2003). V4 (V4v) has been considered to be a center for color processing (Bartels and Zeki, 2000, 2003; Zeki et al., 1991). However, Hadjikhani et al. (1998) discovered an area they labeled V8, located more posterior to V4, that responded to color stimulation. These authors suggest that V8 not V4v are processing color information (Hadjikhani et al., 1998; Tootel et al., 2003, 2004). Future studies will clarify the physiological roles of V4 and V8.

It has been shown that the onset of isoluminant R–G gratings preferentially activates the P pathway (Murray et al., 1987; Porciatti and Sartucci, 1999; Tobimatsu and Kato, 1998; Tobimatsu et al., 1995). Scalp VEPs to the onset of isoluminant R–G pattern showed N120 while high contrast achromatic patterns evoked N95 in the occipital area (Murray et al., 1987; Porciatti and Sartucci, 1999; Tobimatsu, 2002a; Tobimatsu et al., 1995). A few studies investigated the neuromagnetic responses to color stimuli

(Fylan et al., 1997; Regan and He, 1996; Tobimatsu et al., 1999). VEFs to isoluminant color stimuli showed N120m that corresponded to N120 of VEPs. ECDs of N120m were estimated in V1 (Fylan et al., 1997; Tobimatsu et al., 1999) and those of N95m were also generated in V1 (Tobimatsu et al., 1999). Interestingly, the amplitude of N95m was markedly attenuated at the low contrast level (Tobimatsu et al., 1999), suggesting that N120m was specific to color response rather than contrast response.

Processing of facial images has been studied extensively during the past 10 years. Neurophysiological recordings (Allison et al., 1994, 1999; Bentin et al., 1996) and fMRI studies (Downing et al., 2001; Kanwisher et al., 1997; Puce et al., 1996; Tootell et al., 2003) showed that brain areas responsible for facial perception are localized in the fusiform gyri. However, recent neuroimaging studies have revealed that the representations of faces and objects in ventral temporal cortex are widely distributed and overlapping (Hanson et al., 2004; Haxby et al., 2001; Ishai et al., 2005). Bentin et al. (1996) reported that N170 component of VEPs recorded at T5 or T6 was the face-specific response because face images provoked greater responses than other images. In accordance with their hypothesis, ECDs of face-specific VEFs (N170m, latency 140–170 ms) that correspond to N170 have been localized in fusiform gyri with right hemisphere predominance (Fig. 5a) (Linkenkaer-Hansen et al., 1998; Lu et al., 1991; Nakamura et al., 2001; Sams et al., 1997; Swithenby et al., 1998; Watanabe et al., 1999). Similarly, intracranial recording of VEPs to face stimuli have shown that N200 is a face-specific response in the fusiform gyrus (Allison et al., 1994, 1999). The latency difference between N170m (N170 at T5 or T6) and N200 remains unexplained, though it may suggests that the two responses are originated in different neuronal

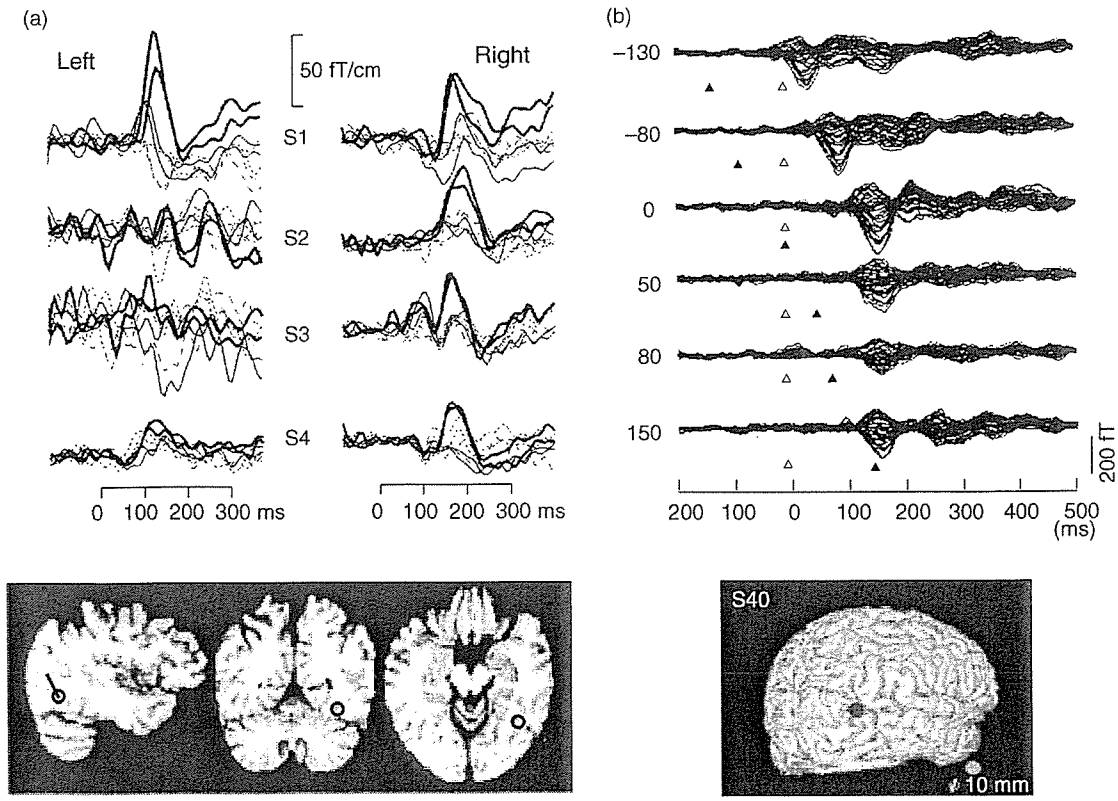

Fig. 5. Neuromagnetic signals of four subjects over the posterior part of the left and right hemispheres (upper column) and ECDs overlaid on MRI of subjects 3 (lower column) (adapted from Sams et al., 1997) (a). Traces from two consecutive recordings are superimposed (upper column). The responses to face stimuli are presented with thick continuous lines. The thinner continuous curves indicate responses to pointillized faces, the thinnest short dashed lines responses to everyday objects and longer dashed lines responses to spheres. Right, back and top view of MRI (lower column, top). The source area (white dot) of the face-specific response is projected onto the surface of the brain along the viewing direction. MRI slices at the source level of the face-specific response (lower column, bottom). The line in the sagittal section shows the direction of the ECD. Time courses of averaged waveforms of 37-ch magnetic responses recorded from the single subject (S10) for each ISI in one direction of the apparent motion (upper column) (adapted from Kawakami et al., 2000) (b). The first component of response with relatively high amplitude was constantly evoked for all the ISI conditions. The peak amplitude of this first component reached a maximums about ISI = 0 ms. The peak latency of the first component was constant for ISI > 0 ms. Although the peak latency from the trigger (turning off of LED 1) decreased for ISI < 0 ms, the interval between the peak and the first visual stimulus (turning on of LED 2) remained constant. Closed triangles indicate the turning on of LED 2, and open triangles the turning off of LED 1. Mean dipole location for a single subject (S40) overlaid on three dimensional brain image of each one (lower column). The image is viewed from the right posterior side. Because the estimated location usually was in the sulcus, the nearest cortical surface is shown by the center of the circle. The area (size) of the circle corresponds to the size of activated cortex estimated for the maximum ECD moment, using the relation 40 mm^2 per 10 nAm.

subgroups. Further studies are necessary to clarify these neural generators. It is interesting to note that age-related increase of N170m latency without prolonged P100m latency has been reported (Nakamura et al., 2001). This finding suggests that the ventral visual pathway, from V1 to V4, is more affected by aging than V1.

5.2. Cortical areas responsive to motion stimuli

Motion perception is mediated by the M pathway and V5/MT is involved in motion processing (Tootell et al., 1995; Uusitalo et al., 1997; Watson et al., 1993). Adjacent to V5 is V5A /MST, which is a region particularly responsive to rotation stimuli (Haug et al., 1998). Visual motion stimuli can be characterized by direction of motion: linear translation, rotation, expansion and contraction, and motion in depth. A special stimulus is the 'random dot' kinematogram, where the overall motion is extracted from a set of coherently and/or incoherently moving subunits. A distinction should also be made among real motion, apparent motion (stepwise dislocation) and illusory motion (motion aftereffect, etc.). All these types of stimuli have been applied in human volunteers to detect the cortical areas involved in the processing and perception of visual motion.

A number of MEG studies have been carried out to relate motion perception to the function of V5/MT. Although neuromagnetic responses vary with types of motion stimuli, most studies have demonstrated that V5/MT has an important role for motion perception (Ahlfors et al., 1999; Anderson et al., 1996; Bakardjian et al., 2002; Bundo et al., 2000; Haug et al., 1998; Kaneoke et al., 1997, 1998; Kawakami et al., 2000, 2002; Lam et al., 2000; Naito et al., 2000; Nakamura et al., 2003; Uusitalo et al., 1997). The speed of motion is encoded in the neural activity of V5/MT in a linear way (Kaneoke et al., 1997, 1998) or nonlinear way (Fig. 5b) (Bakardjian et al., 2002; Kawakami et al., 2002). Incoherent motion is represented in V5/MT neurons to the same degree as coherent motion (Lam et al., 2000). V5/MT has a directional preference for downward versus upward motion in the upper visual field (Naito et al., 2000). The sudden change in the direction of visual motion was found to activate multiple motion-sensitive areas that were temporally overlapping but different characteristic patterns of activity, including V1, V2, V3A, V5/MT, superior temporal sulcus and frontal eye field (Ahlfors et al., 1999).

Jeffreys (1996) examined the influence of a very wide range of different stimulus parameters on VEPs. He has demonstrated that there is parallel processing of depth- and contour-related features of stationary stimuli in anatomically separate regions of the human visual cortex (Jeffreys, 1996). Three-dimensional depth perception can be explored when dynamic random-dot stereograms are presented binocularly (see review for Skrandies, 2001). He has suggested that fewer neurons in V1 are sensitive to horizontal disparity and that higher visual areas like V2 are more engaged with stereoscopic processing. In addition, there is a high correlation between clinical symptoms, perceptual deficiency and altered stereoscopic VEP amplitudes and latencies in patients with selectively disturbed depth perception but normal visual acuity. Namely, the P100 latency and amplitude of monocular PR-VEPs are normal in such patients but the patients with abnormally large disparity thresholds show more prolonged latency and smaller amplitude of stereoscopic VEPs.

6. Feedforward and feedback connections in the visual brain

A single visual stimulus activates neurons in many different cortical areas. However, it has not yet fully understood how the neural activity in these numerous active zones leads to a unified percept of the visual scene. The anatomical basis for these interactions is the dense network of connections that link the visual areas (see Sections 2.2. and 2.3.). Within this network, feedforward connections transmit signals from lower-order areas such as V1 or V2 to higher-order areas. In addition, there is an anatomical evidence of dense web of feedback connections (Bartels and Zeki, 1998; Zeki, 1993). Using reversible inactivation of a higher-order area (monkey V5/MT), Hupé et al. (1998) demonstrated that the feedback connections served to amplify and focus activity of neurons in lower-order areas. Particularly, feedback connections were important in the differentiation of figure from background in the case of low salience stimuli. In accord with this finding, selective attention can influence early sensory processing in the visual cortex (Anllo-Vento et al., 1998; Baas et al., 2002; Di Russo et al., 2003; Gomez Gonzalez et al., 1994; Kenemans et al., 2000; Martínez et al., 2001). Specifically, the CI component (onset at 50–60 ms) was unaffected by attention while the P1 (onset 70–80 ms) and N1 (onset 130–150 ms) components were modulated by attention. This suggests that delayed, reentrant feedback from higher visual areas is present and that may have the function of improving the salience of stimuli at attended locations (Di Russo et al., 2003; Gomez Gonzalez et al., 1994; Martínez et al., 2001).

Recently, several EEG source localization procedures have developed and the inverse problem was solved by introducing reasonable a priori constraints (see for review, Michel et al., 2004). Such technique simultaneously details the temporal and spatial dimensions of brain activity, making it an important and affordable tool to study the properties of neural networks in the visual brain. Using this distributed source localization procedure a more complex source for VEPs was revealed with simultaneous activation of striate and extrastriate areas even at the early processing stages in humans (Morand et al., 2000). This suggests that there is a 'fast bi-directional flow of information' among the different cortical and subcortical areas of the human visual system (Michel et al., 2004; Morand et al., 2000; Pourtois et al., 2004).

We have experienced an interesting case whose VEP findings provide an insight into the presence of feedback system form the extrastriate cortices to V1. This 62-year-old male patient suffered from carbon monoxide intoxication 36 years ago and showed severe visuospatial disturbance with mild visual agnosia but no prosopagnosia. His MRI revealed severe damage to both parieto-ooccipital cortices with V1 sparing (Fig. 6A). His PR-VEPs to 30 min checks were normal (Fig. 6B), however, VEPs to face stimuli (Yamasaki et al., 2004) were abnormal with absence of N80 and P120 at Oz as well as N170 at T5 and T6 (Fig. 6C). The data show that V1 is normally functioning when a simple checkerboard pattern is used but cannot adequately process a complex face stimulus. Feedback connections from higher visual areas may act in a push-pull fashion, amplifying the response to the optimal stimulus for the center mechanism and decreasing that to stimuli activating surround in lower-order areas in monkey (Hupé et al., 1998). Our findings may suggest the presence of the feedback system from extrastriate cortices to V1 in humans. V1, therefore, not only processes early and simple information, it is also involved in middle information processing (Andersson et al., 2004).

7. Clinical applications

7.1. Algorithm for electrodiagnosis of visual pathways' disturbances

Fig. 7 shows the algorithm of sequential steps that can be used to assess visual function in clinical setting (Tobimatsu, 2003). Since detailed description of the recording arrangements and criteria for clinical significant abnormality is beyond the scope of this review, the authors refer the reader to recent reviews on the subject (American Electroencephalographic Society, 1994; Berson, 1994; Celesia, 1984; Celesia and Brigell, 1999b; Celesia et al., 1999; Holder, 2001; Marmor et al., 2004). Electroretinograms (ERGs) are evoked potentials to flashes or pattern stimuli (Bodis-Wollner, 1992; Celesia, 1984; Celesia and Brigell, 1999b; Rimmer and Katz, 1989). Flash ERGs can evaluate the functions of the photoreceptor cells (rods and cones) and Müller cells (Berson, 1994; Marmor et al., in press). Full-field (Ganzfeldt) stimulation should be used while the pupil is maximally dilated. Corneal contact lens electrodes but not skin electrodes are strongly recommended as active recording electrodes (Celesia et al., 1999; Marmor et al., 2004). Pattern ERGs consist of a large positive peak (b-wave or P50) preceded by a small negative peak (N35) and followed by a large negative peak (N95) (Holder, 2001). Pattern ERGs originate from the retinal ganglion cells (Holder, 2001; Maffei and Fiorentini, 1981, 1982; Maffei et al., 1985; Tobimatsu et al., 1989). They are recorded from either corneal contact lens electrodes or conjunctival contact electrodes with natural pupils (Celesia et al., 1999; Holder, 2001; Rimmer and Katz, 1989). The full-field pattern reversal ERGs have been found to be diminished in cases of maculopathy, optic atrophy, optic neuritis, toxic optic neuropathy and ocular hypertension (Bobak et al., 1983; Celesia and Kaufman, 1985; Holder, 2001; Hull and Thompson, 1989; Kaufman and Celesia, 1985; Porciatti and Sartucci, 1996; Porciatti et al., 1997; Rimmer and Katz, 1989). Simultaneous recording of transient pattern ERGs and VEPs provides the retino-cortical time (RCT); time difference between the P100 of the VEP and the b-wave of the ERG (Celesia and Kaufman, 1985; Kaufman and Celesia, 1985). If RCT is normal, even though both the

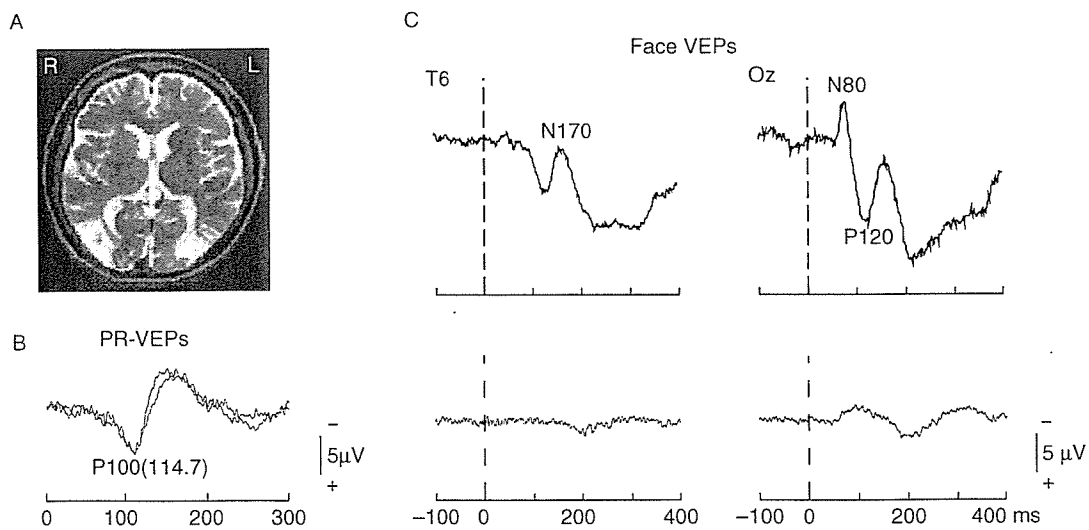

Fig. 6. Brain MRI and VEP findings in a 62-year-old patient with carbon monoxide intoxication due to an explosion of the coal mine 36 years ago. Brain MRI on T2-weighted image shows bilateral parieto-occipital lesions with sparing V1(A). His PR-VEPs to 30 min checks are normal (B). In face VEPs (C), normal subjects show N80 and P120 at Oz and N170 at T6 (upper trace) while these potentials are absent in the patient (lower trace). Decreased sensitivity to the face stimuli resulted from poor feedback connections from higher-order visual areas may cause ill-defined VEP responses.

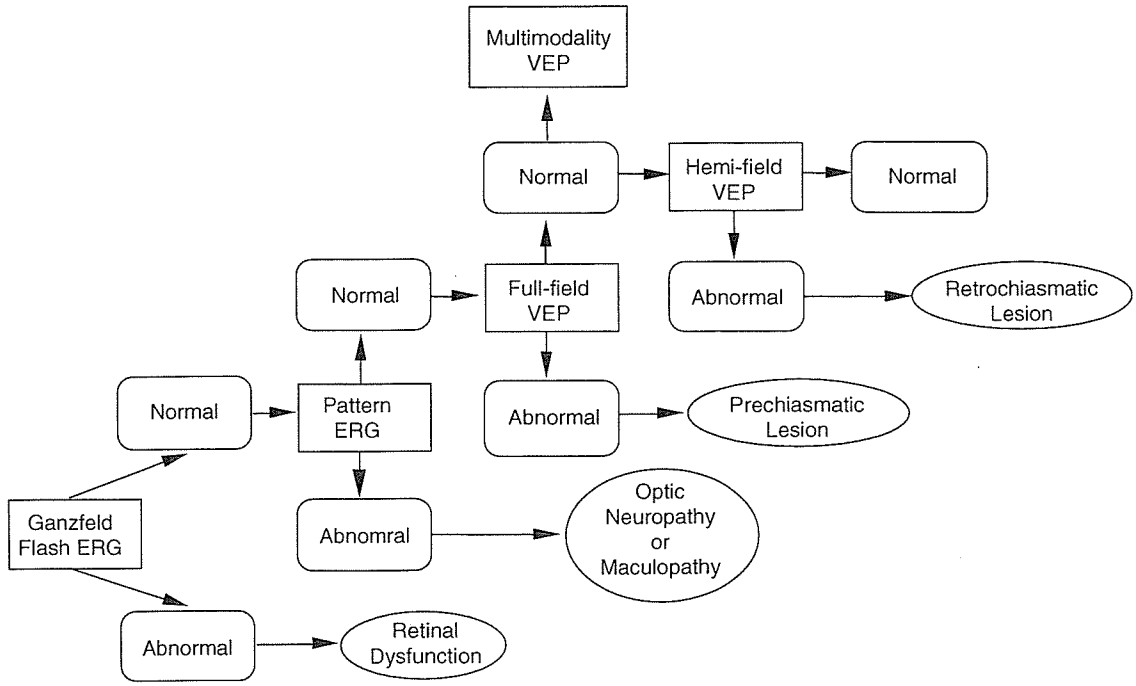

Fig. 7. Algorithm of sequential steps which process visual function. Flash ERGs test the function of retinal receptors and bipolar cells though not exclusively. Pattern ERGs preferentially assesses ganglion cell function. Full-field pattern VEPs usually reflects function of the anterior visual pathways while hemi-field pattern VEPs evaluate the postchiasmal function. Mulitmodality VEPs can assess the functional subdivisions of the visual pathway (Adapted from Tobimatsu, 2003).

ERG and VEP are delayed, the pathology must be intraretinal. If RCT is increased, the pathology must involve conduction defect behind the optic nerve head.

Full-field PR-VEPs are useful in evaluating the function of the anterior visual pathways (Aminoff and Goodin, 1994; Celesia, 1985). The Queen Square System of electrode placement is preferable (American Electroencephalographic Society, 1994; Barrett et al., 1976; Halliday et al., 1972). P100 is the most consistent and least variable peak compared with N75 and N145 and maximal at midoccipital electrode. Monocular abnormality of P100 usually reflects optic nerve or prechiasmal dysfunction. On the other hand, hemi-field pattern VEPs can evaluate the function of the optic radiations and occipital cortex (Aminoff and Goodin, 1994; Celesia, 1985). Hemi-filed stimulation produces asymmetrical amplitude distribution: The greater amplitude of over the scalp ipsilateral to the stimulated field (paradoxical lateralization) is observed (Barrett et al., 1976). Again, P100 is a hallmark like full-filed VEPs, however, the sensitivity of hemi-field VEPs is poor. Their failure to detect the visual field defects is probably due to (1) the topographic variability of the visual cortex in humans and (2) the large cortical representation of the macular region (Celesia, 1984). Daniel and Whitteridge (1961) introduced the concept of cortical magnification factor in monkeys: 5 mm per deg in the foveal area approximately corresponded to 0.25 mm per deg at an eccentricity of 20–30 °. This magnified representation of the central retina was confirmed by the finding that VEP amplitudes were proportional to the cortical area stimulated by scaled stimuli (Baseler et al., 1994; Meredith and Celesia, 1982). Checks greater than 50′ is recommended for hemi-field stimulation to stimulate larger areas of retina outside the foveal region (American Electroencephalographic Society, 1994). To improve the diagnostic yield of hemi-filed VEPs, it is necessary to develop the methods to preferentially stimulate the peripheral visual fields. This limitation could be overcome by using the multiple-input method in which 60 or more local VEP responses, called multifocal VEPs, could be obtained over a wide retinal area if the stimulus array was scaled to account for cortical magnification (Baseler et al., 1994). Multifocal VEPs might allow us to uncover the visual field defect because the recent advances in the recording technique (Fortune and Hood, 2003; James, 2003; Klistorner et al., 1998).

7.2. *Multimodality VEPs*

As previously mentioned, the visual system analyzes spatial, temporal and chromatic aspects of objects via multiple, parallel channels. Disease states may alter the function of only some of these parallel channels, leaving others intact. Study of responses to multimodal visual stimuli more adequately assesses the visual system than using only PR-VEPs, in which stimulus parameters such as contrast, luminance, and spatial and temporal frequencies are fixed (Chiappa, 1997). Previous studies have shown that the use of multiple check sizes gives a higher

yield of abnormalities than use of a single check size (Hughes et al., 1987; Novak et al., 1988; Oishi et al., 1985). Similarly, the combined use of transient and steady-state VEPs increases the abnormality rate in patients with MS and optic neuritis (Bobak et al., 1988b; Celesia et al., 1992). Abnormal PR-VEPs and a reduction in the contrast sensitivity function may be present in patients with Parkinson's disease (PD), and delayed VEPs, if present, can be shortened by levodopa therapy (Bodis-Wollner, 1990). PD patients show a temporal frequency-dependent VEP changes with a selective deficit in response to 4 Hz stimuli (8 reversals/s) (Marx et al., 1986). At least some of the deficit relate to impaired center-surround interaction of neurons in the retina caused by systemic dopaminergic deficiency (Bodis-Wollner, 1990, 1992). Dopamine deficiency may decrease surround inhibition and increase the area of signal summation for the ganglion cell at the expense of decreasing total

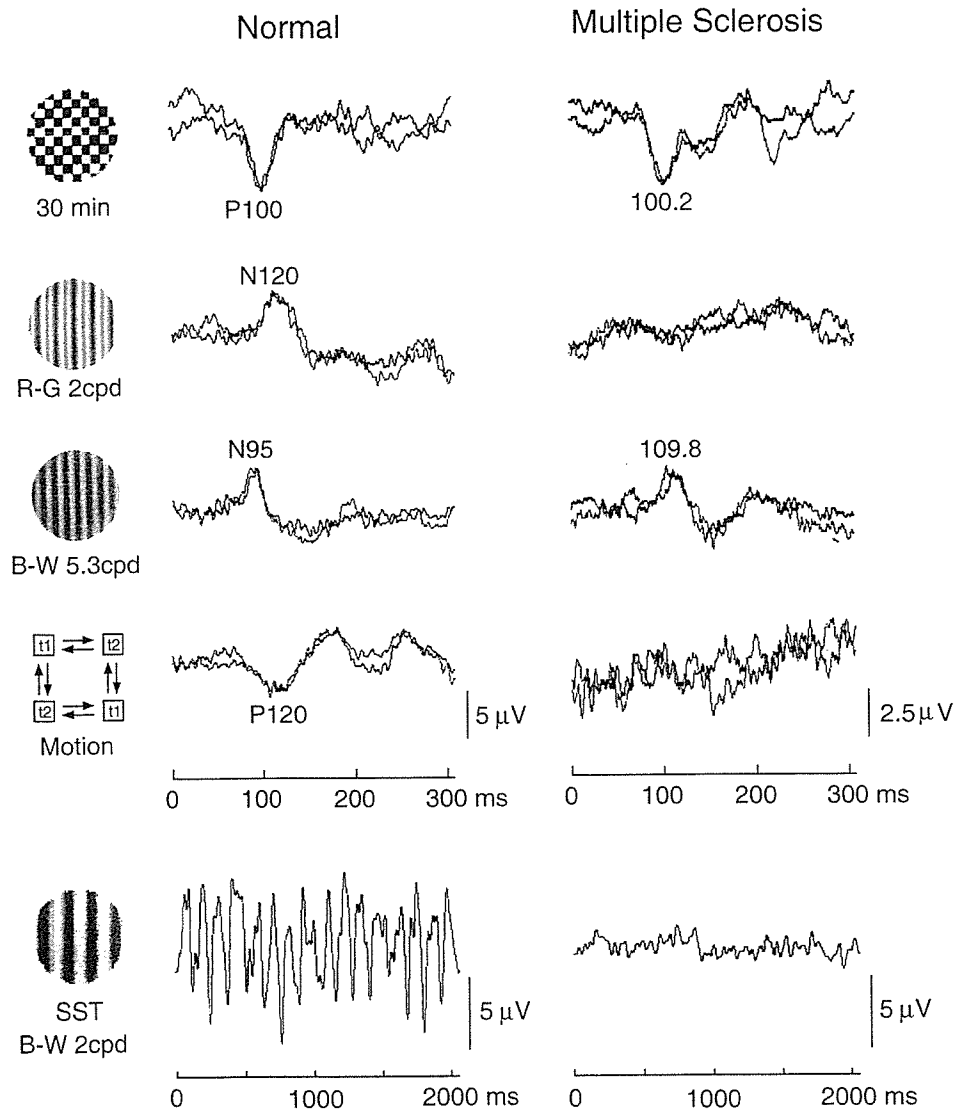

Fig. 8. Multimodality VEPs in a normal subject (left column) and a patient with multiple sclerosis (right column). A checkerboard pattern consisted of 30 min checks of high contrast (90%) which was phase-reversed at a rate of 1 Hz for recording transient PR-VEPs (top). The mean luminance was 180 cd/m^2. Isoluminant chromatic sinusoidal gratings (red–green) at 2 cpd appeared for 200 ms and were replaced by a yellowish background for 800 ms in recording chromatic pattern appearance VEPs (second row). High contrast (90%) achromatic sinusoidal gratings (black–white) at 5.3 cpd also appeared for 200 ms and were replaced by a grayish white background for 800 ms for recording achromatic VEPs (third row). The mean luminance of chromatic and achromatic gratings was 16 cd/m^2. An apparent motion display was used to record motion VEPs (fourth row). Two squares (60 min of arc, t1) at opposite corners of a hypothetical square were presented together for a duration of 500 ms and then switched off, followed by two squares (t2) appearing simultaneously on the remaining two corners. Moreover, high contrast (90%) achromatic gratings at 2 cpd were reversed at a rate of 4 Hz (8 reversals/s) for recording S-VEPs (bottom). The patient shows normal P100 and N95 with absent N120 and P120. A reduced response of S-VEPs is evident (bottom). Abbreviations: cpd: cycles/deg; R–G, red–green sinusoidal gratings; B–W, black–white sinusoidal gratings; Motion, apparent motion; SST, steady-state.

Table 1
Proportion of abnormal tests with symptomatic ($n=8$) or asymptomatic ($n=19$) eyes

	Checks	R–G	B–W	Motion	SST	All combined
No. of symptomatic eyes with abnormal response	5 (62.5)	6 (75.0)	7 (87.5)	4 (50.0)	6 (75.0)	8 (100)
No. of asymptomatic eyes with abnormal response	5 (26.3)	3 (15.8)	9 (47.4)	4 (21.1)	8 (42.1)	12 (63.2)
Total	10 (37.0)	9 (33.3)	16 (59.3)	8 (29.6)	14 (51.9)	20 (74.1)

Symptomatic eyes: patients exhibited visual symptoms or had a history of optic neuritis. Asymptomatic eyes: patients were visually asymptomatic. Percentages appear in parentheses.

response gain. Thus, perception of the spatio-temporal information of the visual stimuli is disturbed in PD (Bodis-Wollner, 1990; Peppe et al., 1998; Sartucci et al., 2003). Interestingly, temporal frequency deficit was also observed in senile dementia of the Alzheimer type by using S-VEPs to LED goggle stimulation (Tobimatsu et al., 1994). This phenomenon may be explained by pathology that affects the early stage of visual signal processing (Arakawa et al., 1997). Although normal flash but abnormal pattern ERGs (Katz et al., 1989; Sadun and Bassi, 1990) are consistent with the involvement of the retinal ganglion cells, abnormal flash but normal pattern VEPs with normal pattern ERGs imply the extra-geniculo-striatal pathology (Kergoat et al., 2002; Philpot et al., 1990; Rizzo et al., 1992) in Alzheimer's disease. A decrease in acethylcholine in the widespread areas of the brain may underlie the temporal frequency attenuation because the cholinergic system plays an integral role in transmission of visual information (Arakawa et al., 1993; Bajalan et al., 1986; Sato et al., 1987).

Tobimatsu and Kato (1998) introduced multimodality VEPs to assess the functions of multiple, parallel visual pathways. Since testing multimodal visual stimuli is time-consuming, techniques must be optimized to detect pathology. Five different modalities were tested and optimal stimulus conditions were selected, thus it was possible to use the technique clinically because it was reliable and quick (Kurita-Tashima et al., 1991; Tobimatsu et al., 1993b, 1995, 1996). The five different modalities of visual stimulation were (Fig. 8): T-VEPs to 30′ checkerboard patterns, isoluminant R–G and high contrast B–W sinusoidal gratings and apparent motion stimulation, and S-VEPs to B–W gratings. The morphology of VEPs is altered by the physical attributes of the visual stimuli. Multimodality VEPs were recorded in 15 normal controls and 14 patients with optic neuritis most of whom were diagnosed with MS to test the hypothesis that these potentials may preferentially test different visual pathways. VEPs to 30′ checks were abnormal in 7 patients (or 10 eyes), however, considering all five modalities, abnormal responses were seen in 12 patients (or 20 eyes). Abnormality rates were not equal among the visual stimuli (Table 1), which thus suggested possible dysfunction of individual subdivisions in the visual pathways.

7.3. VEPs associated with texture segregation

The segregation of visual scenes based on contour information is a fundamental process of early vision. In natural scenes, contour boundaries are mainly extracted on the basis of simple cues, such as luminance, color, or motion, but they can also be defined by more complex cues, such as texture or illusory contours (Kastner et al., 2000; Ohtani et al., 2002). VEPs associated with texture segregation (tsVEPs) have been reported (Bach and Meigen, 1992, 1997; Bach et al., 2000; Fahle et al., 2003; Lamme et al., 1992; Romani et al., 2003). Earlier studies of normal texture segregation have revealed a negative component peaking at around 150–200 ms in response to textures stimuli (Bach and Meigen, 1992, 1997). This component is thought to originate from V1 and to reflect the integration of information from associative visual areas (V2 and V3) via intracortical retroaction circuits towards V1 (Bach and Meigen, 1992, 1997; Lamme et al., 1992). tsVEPs are of interest because they provide an intermediate measure of visual processing between low-level VEPs (or pattern VEPs), which culminate at around 100 ms, and cognitive ones which peak typically after 300 ms. Recently, Lachapelle et al. (2004) have demonstrated that tsVEPs are sensitive to traumatic brain injury and can help quantify cortical damage that is not revealed with pattern VEPs. Therefore, tsVEPs reflect a complex level of visual information processing and could be used to infer more global information processing integrity in the brain than pattern VEPs.

8. Conclusions

The physical natures of the visual stimuli are coded by several separate and parallel pathways at multiple sites in the visual system. In this review, emphasis has been placed on the understanding of the physiological and functional organizations of the visual pathways. VEPs are an important means of obtaining reproducible, quantitative data on the function of the visual pathways. The authors believe that modulating the attributes of the visual stimuli could enable researchers to explore the human visual function from the retina to higher cortical visual areas. Spatio-temporal analysis of visual information processing could provide

data on the feedforward and feedback connections of the visual cortices.

Acknowledgements

This study was supported in part by Grant-in-Aid for the 21st Century COE Program and Grant-in-Aid for Scientists, No 16390253 and No 16200005 from the Ministry of Education, Culture, Sports, Science and Technology in Japan.

References

Ahlfors SP, Simpson GV, Dale AM, Belliveau JW, Liu AK, Korvenoja A, Virtanen J, Huotilainen M, Tootell RBH, Aronen HJ, Ilmoniemi RJ. Spatiotemporal activity of a cortical network for processing visual motion revealed by MEG and fMRI. J Neurophysiol 1999;82: 2545–55.

Aine CJ, Bodis-Wollner I, George JS. Generators of visually evoked neuromagnetic responses. Spatial-frequency segregation and evidence for multiple sources. In: Sato S, editor. Advances in neurology. Magnetoencephalography, vol. 54. New York: Raven Press; 1990. p. 141–55.

Aine CJ, Supek S, George JS. Temporal dynamics of visual-evoked neuromagnetic sources: effects of stimulus parameters and selective attention. Int J Neurosci 1995;80:79–104.

Aine C, Huang M, Stephen J, Christner R. Multistart algorithms for MEG empirical data analysis reliably characterize locations and time courses of multiple sources. NeuroImage 2000;12:159–72.

Allison T, Hume AL, Wood CC, Goff WR. Developmental and aging changes in somatosensory, auditory and visual evoked potentials. Electroencephalogr Clin Neurophysiol 1984;58:14–24.

Allison T, Ginter H, McCarthy G, Nobre AC, Puce A, Luby M, Spencer DD. Face recognition in human extrastriate cortex. J Neurophysiol 1994;71:821–5.

Allison T, Puce A, Spencer DD, McCarthy G. Electrophysiological studies of human face perception. I: potentials generated in occipitotemporal cortex by face and non-face stimuli. Cereb Cortex 1999;9:415–30.

American Electroencephalographic Society guidelines on evoked potentials: guideline nine: guidelines on evoked potentials. J Clin Neurophysiol 1994;11:40–73.

Aminoff MJ, Goodin DS. Visual evoked potentials. J Clin Neurophysiol 1994;11:493–9.

Amunts K, Malikovic A, Mohlberg H, Schormann T, Zilles K. Brodmann's areas 17 and 18 brought into stereotaxic space—where and how variable? NeuroImage 2000;11:66–84.

Anderson SJ, Holliday IE, Singh KD, Harding GFA. Localization and functional analysis of human cortical area V5 using magneto-encephalography. Proc R Soc Lond B 1996;263:423–31.

Andersson F, Etard O, Denise P, Petit L. Early visual evoked potentials are modulated by eye position in humans induced by whole body rotations. BMC Neurosci 2004;519:35.

Anllo-Vento L, Luck SJ, Hillyard SA. Spatio-temporal dynamics of attention to color: evidence from human electrophysiology. Hum Brain Mapp 1998;6:216–38.

Arakawa K, Peachey NS, Celesia GG, Rubboli G. Component-specific effects of physostigmine on the cat visual evoked potential. Exp Brain Res 1993;95:271–6.

Arakawa K, Tobimatsu S, Kato M, Kobayashi T. Different effects of cholinergic agents on responses recorded from the cat visual cortex and lateral geniculate nucleus dorsalis. Electroencephalogr Clin Neurophysiol 1997;104:375–80.

Arakawa K, Tobimatsu S, Kurita-Tashima S, Nakayama M, Kira J-I, Kato M. Effects of stimulus orientation on spatial frequency function of the visual evoked potential. Exp Brain Res 2000;131:121–5.

Baas JMP, Kenemans JL, Mangun GR. Selective attention to spatial frequency: an ERP and source localization analysis. Clin Neurophysiol 2002;113:1840–54.

Bach M, Meigen T. Electrophysiological correlates of texture segregation in the human visual evoked potential. Vision Res 1992;32:417–24.

Bach M, Meigen T. Similar electrophysiological correlates of texture segregation induced by luminance, orientation, motion and stereo. Vision Res 1997;37:1409–14.

Bach M, Schmitt C, Quenzer T, Meigen T, Fahle M. Summation of texture segregation across orientation and spatial frequency: electrophysiological and psychophysical findings. Vision Res 2000;40:3559–66.

Bajalan AAA, Wright CE, van der Vliet VJ. Changes in the human visual evoked potential caused by the anticholinergic agent hyoscine hydrobromide: comparison with results in Alzheimer's disease. J Neurol Neurosurg Psychiatry 1986;49:175–82.

Bakardjian H, Uchida A, Endo H, Takeda T. Magnetoencephalographic study of speed-dependent responses in apparent motion. Clin Neurophysiol 2002;113:1586–97.

Baker CL, Hess RF, Zihl J. Residual motion perception in a 'Motion-Blind' patient, assessed with limited-lifetime random dot stimuli. J Neurosci 1991;11:454–61.

Barrett G, Blumhardt L, Halliday AM, Halliday E, Kriss A. A paradox in the lateralisation of the visual evoked response. Nature 1976;261: 253–5.

Bartels A, Zeki S. The theory of multistage integration in the visual brain. Proc R Soc Lond B 1998;265:2327–32.

Bartels A, Zeki S. The architecture of the colour centre in the human visual brain: new results and a review. Eur J Neurosci 2000;12:172–93.

Barton JS, Sharpe JA. Motion direction discrimination in blind hemifields. Ann Neurol 1997;41:255–64.

Baseler HA, Sutter EE, Klein SA, Carney T. The topography of visual evoked response properties across the visual field. Electroencephalogr Clin Neurophysiol 1994;90:65–81.

Bentin S, Allison T, Puce A, Perez E, McCarthy G. Electrophysiological studies of face perception in humans. J Cogn Neurosci 1996;8: 551–65.

Berson EL. Visual function testing: clinical correlations. J Clin Neurophysiol 1994;11:472–81.

Blakemore C, Campbell FW. On the existence of neurones in the human visual system selectively sensitive to the orientation and size of retinal images. J Physiol 1969;203:237–60.

Bobak P, Bodis-Wollner I, Harnois C, Maffei L, Mylin L, Podos S, Thornton J. Pattern electroretinograms and visual-evoked potentials in glaucoma and multiple sclerosis. Am J Ophthalmol 1983;96:72–83.

Bobak P, Yates D, Goodwin J, Morrison R. Steady-state visual evoked potentials to asymmetrical contrast. Curr Eye Res 1988a;7:265–75.

Bobak P, Friedman R, Brigell M, Goodwin J, Anderson R. Visual evoked potentials to multiple temporal frequencies. Use in the differential diagnosis of optic neuropathy. Arch Ophthalmol 1988b;106:936–40.

Bodis-Wollner I. Visual deficits related to dopamine deficiency in experimental animals and Parkinson's disease patients. Trends Neurosci 1990;13:296–302.

Bodis-Wollner I. Sensory evoked potentials: PERG, VEP, and SEP. Curr Opin Neurol Neurosurg 1992;5:716–26.

Bodis-Wollner I, Hendley CD. Relation of evoked potentials to pattern and local luminance detectors in the human visual system. In: Desmedt JE, editor. Visual evoked potentials in man: new developments. Oxford: Clarendon Press; 1977. p. 197–207.

Bodis-Wollner I, Hendley CD, Atkin A. Evaluation by evoked potentials of dissociated visual functions in patients with cerebral lesions. In: Desmedt JE, editor, Visual evoked potentials in man: new developments. Oxford: Clarendon Press; 1977. p. 514–524.

Bodis-Wollner I, Ghilardi MF, Mylin LH. The importance of stimulus selection in VEP practice: the clinical relevance of visual physiology. In: Cracco RQ, Bodis-Wollner I, editors. Evoked potentials. New York: Alan R Liss; 1986. p. 15–27.

Brigell M, Bach M, Barber C, Moskowitz A, Robson J. Guidelines for calibration of stimulus and recording parameters used in clinical electrophysiology of vision. Doc Ophthalmol 2003;107:185–93.

Bundo M, Kaneoke Y, Inao S, Yoshida J, Nakamura A, Kakigi R. Human visual motion areas determined individually by magnetoencephalography and 3D magnetic resonance imaging. Hum Brain Mapp 2000; 11:33–45.

Butler SR, Georgiou GA, Glass A, Hancox RJ, Hopper JM, Smith KRH. Cortical generators of the CI component of the pattern-onset visual evoked potential. Electroencephalogr Clin Neurophysiol 1987;68: 256–67.

Camisa J, Mylin LH, Bodis-Wollner I. The effect of stimulus orientation on the visual evoked potential in multiple sclerosis. Ann Neurol 1981;10: 532–9.

Campbell FW, Maffei L. Electrophysiological evidence for the existence of orientation and size detectors in the human visual system. J Physiol 1970;207:635–52.

Casagrande VA, Royal DW. Parallel visual pathways in a dynamic system. In: Kaas JH, Collins CE, editors. The primate visual system. London: CRC Press; 2003. p. 1–27.

Casagrande VA, Xu X. Parallel visual pathways: a comparative perspective. In: Chalupa L, Werner JS, editors. The visual neurosciences. Cambridge, MA: MIT Press; 2004. p. 494–506.

Celesia GG. Evoked potential techniques in the evaluation of visual function. J Clin Neurophysiol 1984;1:55–76.

Celesia GG. Visual evoked responses. In: Owen JH, Davis H, editors. Evoked potential testing. Orlando, FL: Grune & Stratton; 1985. p. 1–54.

Celesia GG. Anatomy and physiology of the visual pathways and cortex. In: Celesia GG, editor. Disorders of visual processing, handbook of clinical neurophysiology, vol. 5. Amsterdam: Elsevier; 2005. p. 143–66.

Celesia GG, Brigell MG. Cortical blindness and visual processing. Electroencephalogr Clin Neurophysiol 1999a;S49:133–41.

Celesia GG, Brigell MG. Recommended standards for pattern electroretinograms and visual evoked potentials. Electroencephalogr Clin Neurophysiol 1999b;S52:53–67.

Celesia GG, DeMarco Jr PJ. Anatomy and physiology of the visual system. J Clin Neurophysiol 1994;11:482–92.

Celesia GG, Kaufman D. Pattern ERGs and visual evoked potentials in maculopathies and optic nerve diseases. Invest Ophthalmol Vis Sci 1985;26:726–35.

Celesia GG, Kaufman D, Cone S. Effects of age and sex on pattern electroretinograms and visual evoked potentials. Electroencephalogr Clin Neurophysiol 1987;68:161–71.

Celesia GG, Brigell M, Gunnink R, Dang H. Spatial frequency evoked visuograms in multiple sclerosis. Neurology 1992;42:1067–70.

Celesia GG, Peachey NS, Brigell M, DeMarco Jr PJ. Visual evoked potentials: recent advances. Electroencephalogr Clin Neurophysiol 1996;S46:3–14.

Celesia GG, Brigell MG, Vaphiades MS. Hemianopic anosognosia. Neurology 1997;49:88–97.

Celesia GG, Brigell MG, Peachey N. Recommended standards for electroretinograms. Electroencephalogr Clin Neurophysiol 1999;S52: 45–52.

Chatterjee S, Callaway EM. Parallel colour-opponent pathways to primary visual cortex. Nature 2003;426:668–71.

Chiappa KH. Evoked potentials in clinical medicine. Philadelphia, PA/New York: Lippincott/Raven; 1997. p. 31–94.

Dacey DM. Primate retina: cell types, circuits and color opponency. Prog Retin Eye Res 1999;18:737–63.

Dacey DM, Packer OS. Colour coding in the primate retina: diverse cell types and cone-specific circuitry. Curr Opin Neurobiol 2003;13:421–7.

Daniel PM, Whitteridge D. The representation of the visual field on the cerebral cortex in monkeys. J Physiol 1961;159:203–21.

De Monasterio FM, Gouras P. Functional properties of ganglion cells of the rhesus monkey retina. J Physiol 1975;251:167–95.

De Valois KK, De Valois RL, Yund EW. Responses of striate cortex cells to grating and checkerboard patterns. J Physiol 1979;291:483–505.

De Yoe EA, Felleman DJ, Van Essen DC, McClendon E. Multiple processing streams in occipitotemporal visual cortex. Nature 1994;371: 151–4.

De Yoe EA, Carman GJ, Bandettini P, Glickman S, Wieser J, Cox R, Miller D, Neitz J. Mapping striate and extrastriate visual areas in human cerebral cortex. Proc Natl Acad Sci USA 1996;93:2382–6.

Derrington AM, Krauskopf J, Lennie P. Chromatic mechanisms in lateral geniculate nucleus of macaque. J Physiol 1984;357:241–65.

Di Russo F, Martínez A, Sereno MI, Pitzalis S, Hillyard SA. Cortical sources of the early components of the visual evoked potential. Hum Brain Mapp 2001;15:95–111.

Di Russo F, Martínez A, Hillyard SA. Source analysis of event-related cortical activity during visuo-spatial attention. Cereb Cortex 2003;13: 486–99.

Di Russo F, Pitzalis S, Spitoni G, Aprile T, Patria F, Spinelli D, Hillyard SA. Identification of the neural sources of the pattern-reversal VEP. NeuroImage 2005;24:874–86.

Downing PE, Jiang Y, Shuman M, Kanwisher N. A cortical area selective for visual processing of the human body. Science 2001;293:2470–3.

Enroth-Cugell C, Robson JG. The contrast sensitivity of retinal ganglion cells of the cat. J Physiol 1966;187:517–52.

Fahle M, Quenzer T, Braun C, Spang K. Feature-specific electrophysiological correlates of texture segregation. Vision Res 2003;43:7–19.

Felleman DJ, Van Essen DC. Distributed hierarchical processing in the primate cerebral cortex. Cereb Cortex 1991;1:1–47.

Ferrera VP, Nealey TA, Maunsell JHR. Mixed parvocellular and magnocellular geniculate signals in visual area V4. Nature 1992;358: 756–8.

Ferrera VP, Nealey TA, Maunsell JHR. Responses in macaque visual area V4 following inactivation of the parvocellular and magnocellular LGN pathways. J Neurosci 1994;14:2080–8.

Fortune B, Hood DC. Conventional pattern-reversal VEPs are not equivalent to summed multifocal VEPs. Invest Ophthalmol Vis Sci 2003;44:1364–75.

Fylan F, Holliday IE, Singh KD, Anderson SJ, Harding GFA. Magnetoencephalographic investigation of human cortical area V1 using color stimuli. NeuroImage 1997;6:47–57.

Gomez Gonzalez CM, Clark VP, Fan S, Luck SJ, Hillyard SA. Sources of attention-sensitive visual event-related potentials. Brain Topogr 1994; 7:41–51.

Hadjikhani N, Liu AK, Dale AM, Cavanagh P, Tootell RBH. Retinotopy and color sensitivity in human visual cortical area V8. Nat Neurosci 1998;1:235–41.

Halliday AM, McDonald WI, Mushin J. Delayed visual evoked response in optic neuritis. Lancet 1972;1:982–5.

Hämäläinen M, Hari R, Ilmoniemi RJ, Knuutila J, Lounasmaa OV. Magnetoencephalography—theory, instrumentation, and applications to noninvasive studies of the working human brain. Rev Modern Phys 1993;65:413–97.

Hanson SJ, Matsuka T, Haxby JV. Combinatorial codes in ventral temporal lobe for object recognition: Haxby (2001) revisited: is there a 'face' area? NeuroImage 2004;23:156–66.

Harter MR, White CT. Evoked cortical responses to checkerboard patterns: effect of check-size as a function of visual acuity. Electroencephalogr Clin Neurophysiol 1970;28:48–54.

Hashimoto T, Kashii S, Kikuchi M, Honda Y, Nagamine T, Sibasaki H. Temporal profile of visual evoked responses to pattern-reversal stimulation analyzed with a whole-head magnetometer. Exp Brain Res 1999;125:375–82.